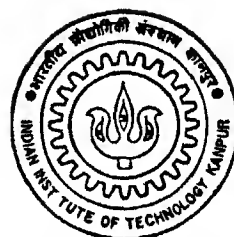


FABRICATION OF A FIBER - OPTIC TRANSVERSAL FILTER

By
TAPAN RAY

EE
1995
M
RAY
FAB



DEPARTMENT OF ELECTRICAL ENGINEERING

INDIAN INSTITUTE OF TECHNOLOGY KANPUR

MAY, 1995

FABRICATION OF A FIBER-OPTIC TRANSVERSAL FILTER

*A Thesis Submitted
in Partial Fulfilment of the Requirements
for the Degree of
MASTER OF TECHNOLOGY*

by

Tapan Ray

to the

DEPARTMENT OF ELECTRICAL ENGINEERING
INDIAN INSTITUTE OF TECHNOLOGY KANPUR

May, 1995

1711180
CENTRAL LIBRARY
IIT KANPUR
Rec. No. A - 121324

EE-1PP5-M-RAY-FAB



A121324

Certificate

It is certified that the work entitled FABRICATION OF A FIBER OPTIC TRANSVER SAL FILTER, by Tapan Ray has been carried out under my supervision and that this work has not been submitted elsewhere for a degree



Dr. Anjan K. Ghosh

Professor,

Department of Electrical Engineering
IIT Kanpur

29 May, 1995

Dedicated

to

my brother

Acknowledgements

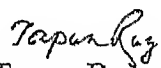
I would like to express my deep sense of gratitude to Dr Anjan K Ghosh for his constant encouragement Only because of his constant support I have been able to complete this work

I am grateful to Dr Joseph John who helped me to carry out the experimental part of my work

I would like to thank all my M Tech batchmates for the memorable moments that we all had together Also I would specially like to thank Jit, Manas Anand, Sudarshan and Santanu for helping me out of difficulties during the preparation of the thesis report and provided me mental support from time to time

My stay here was possible due to the constant moral support provided by my family

May 29, 1995


Tapan Ray

Abstract

A fiber optic finite impulse response transversal filter is fabricated using fiber bundles. The structure is designed to provide low pass filtering action with a bandwidth of 10 MHz. The effects of non uniform illumination of fibers in the bundle and bending losses on the frequency response of the filter are studied. The frequency response of the fabricated filter is measured and is found to be in good agreement with the theoretical frequency response.

Contents

1	Introduction	1
1 1	Advantages of fiber optic signal processing	1
1 2	Past work	2
1 3	Objective of the present work	5
1 4	Overview	5
2	Transversal Filters	6
2 1	Fiber optic transversal filter	7
2 2	Calculation of lengths	8
3	Experiment And Discussions	10
3 1	Experimental set up	10
3 2	Fiber bundle preparation	12
3 3	Causes of non ideal response and their effects	13
3 3 1	Non uniform coupling effect	14
3 3 2	Bending loss and fiber attenuation effect	22
3 3 3	Attenuations of signal due to fiber loss	25
3 3 4	Transmitter and Receiver circuits bandwidth limitations	25
3 4	Experimental Results	28
4	Applications of fiber optic tapped delay line devices	33
4 1	Code generation and matched filtering application	33
4 2	Fiber optic adaptive filters and equalizers	34
4 3	Spread spectrum fiber optic local area network using optical processing	36
4 4	Spectral analysis of radio frequency signals	37

4.5 Transversal filter realization with non uniform tap spacings 38

5 Conclusions 39

List of Figures

1 1	Recirculating delay Line	3
1 2	Tapped delay Line	3
1 3	FIR fiber filter composed of input splitter and output combiner	4
1 4	Fiber bundle approach	5
2 1	Transversal filter structure	6
2 2	Cross sectional view of the fiber bundle at the ends	8
2 3	Ideal frequency response of the fiber optic filter	9
3 1	Experimental set up for measuring the frequency response of the fiber optic transversal filter	11
3 2	Light emitting diode, model MFOE71	11
3 3	Spherical coordinate system	14
3 4	Driver circuit of the LED to measure the far field pattern	16
3 5	Experimental set up for measuring the far field pattern of the LED	17
3 6	Far field pattern of LED in ϕ direction	19
3 7	Far field pattern of LED in θ direction	19
3 8	Inside dimensional details of coupling between LED and the fiber bundle	20
3 9	Coupling loss effect on the frequency response of the filter (cle3 is the response when $x=3$ mm, cle5 is the response when $x=5$ mm)	22
3 10	Bending loss effect on filter frequency response, loop dia=10 cm (ble10 is the response considering the bending loss)	24
3 11	Bending loss effect on filter frequency response, loop of dia=15 cm (ble15 is the response considering the bending loss)	25
3 12	Combined frequency response of transmitter and receiver circuit	26

3 13 Transmitter and Receiver effect on frequency response (tre is the response considering the transmitter and receiver effect)	27
3 14 Expected fiber optic filter frequency response, d=10 cm and x=4 mm	27
3 15 Expected fiber optic filter frequency response d=15 cm and x=4 mm	28
3 16 Comparison between the experimental plot with theoretical one d=15 cm x=4 mm, all h_i 's=1	29
3 17 Relative percentage error between the experimental curve and the theoretical curve	31
3 18 Comparison between the experimental plot with theoretical one d=15 cm, x=4 mm, $h_2=h_4=h_6=0$ other h_i 's=1	31
3 19 Comparison between the experimental plot with theoretical one d=10 cm, x=4 mm, all h_i 's=1	32
3 20 Comparison between the experimental plot with theoretical one, d=10 cm x=4 mm, $h_3=h_5=0$, other h_i 's=1	32
4 1 Block diagram of a fiber optic code generator	34
4 2 Block diagram of a tapped delay line adaptive filter	35
4 3 Block diagram of a fiber optic adaptive filter	35
4 4 Block diagram of a CDMA processor	36
4 5 Block diagram of a system using both optical data encoding and decoding	37
4 6 Block diagram of a tapped delay line spectrum analyzer	38

List of Tables

1 1	Comparison of delay line technology	2
3 1	Far field radiation measurement data of LED	18
3 2	Fractional powers for different values of x	21
3 3	Values of δ_e for different x	21
3 4	Bending loss measurement for diameter of curvature = 15 cm	23
3 5	Bending loss measurement for diameter of curvature = 10 cm	23
3 6	Values of δ_b	24

Chapter 1

Introduction

The use of optical fibers in different areas of science and technology is gaining increasing acceptance because of their attractive features such as large time bandwidth products, extremely low loss, compact light weight devices and insensitivity to interference and crosstalk. The primary application of an optical fiber is to use it as a signal transmission media in a communication system. Recent advances in fiber optics technology has enabled us to consider it to perform a variety of signal processing and sensing operations. The signal processing operations which are possible using optical fibers include convolution, correlation, code sequence generation, matrix vector multiplication, frequency filtering and many others.

1.1 Advantages of fiber optic signal processing

In fiber optic signal processing technology, a lightwave signal is processed optically before its transduction to the electrical form. Optoelectronic conversion contributes loss of energy, so all optical is an advantage. This also eliminates the need for intermediate electronic filtering required in conventional approaches for processing lightwave signals. Hence one can extend the speed and bandwidth capabilities to levels beyond those of the traditional microelectronic circuits which do not have the adequate speed for real time processing of broadband signals. In table 1.1, a comparison of speeds of a few popular techniques is shown.

In case of optical fiber, dispersion of signal limits the attainable bandwidth. Using step index multimode fibers, bandwidth typically in the range of a few MHz km to several

S1 No	Name of Scheme	Operating frequency	Ref
1	Charge coupled device using metal on silicon (MOS) technique	Below 10 MHz	[1]
2	Acoustic wave delay lines	Several hundred Megahertz	[2] [3]
3	Magnetostatic wave devices	2 12 GHz	[4]
4	Super conducting Delay lines	Approx 20 GHz	[5]

Table 1 1 Comparison of delay line technology

hundred MHz km is attainable. The bandwidth is increased using graded index fibers. We can go for even higher bandwidth (greater than 3GHz km) by using signal mode fiber and operating it with a wavelength at which the dispersion is minimum.

Another advantage of using fiber is low loss. The technology of preparing glass fiber is improved to such an extent that even a mere loss of 0.15 dB/km (at 1.55 micrometre wavelength) is attainable. Comparing this with the losses of other delay mediums [6], we see that low loss optical fibers are far superior (for frequencies above 1 GHz) to any practical alternative currently available. However, for frequencies below 1 GHz, acoustic wave devices are attractive in terms of loss [7].

1 2 Past work

The use of optical fiber as a delay medium for signal processing applications was proposed by Wilner and Vanden Hauvel in 1976 [6]. Since then, several ways of realizing a fiber optic delay line processor were proposed and implemented. Two basic delay line structures used in fiber optic signal processing are recirculating delay line [fig 1 1] and non recirculating or tapped delay line [fig 1 2]. The recirculating delay line consists of a loop of fiber which is closed upon itself with a fiber directional coupler. Signals introduced into one end of the delay line circulate around the loop repeatedly and produce outputs on each transit [7]. Recirculating delay lines can be used for data rate transformations [8], uniform pulse train generation [9], and frequency filtering [10]. One disadvantage of recirculating delay line

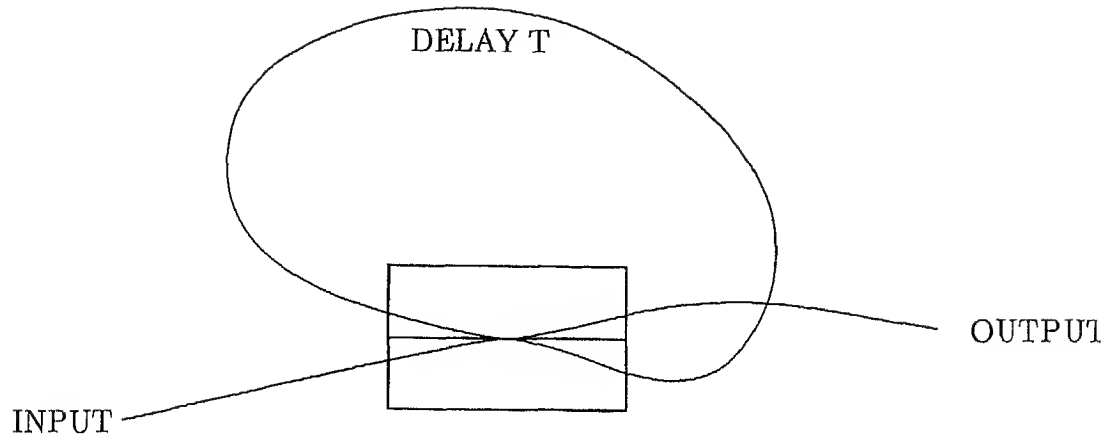


Figure 1.1 Recirculating delay Line

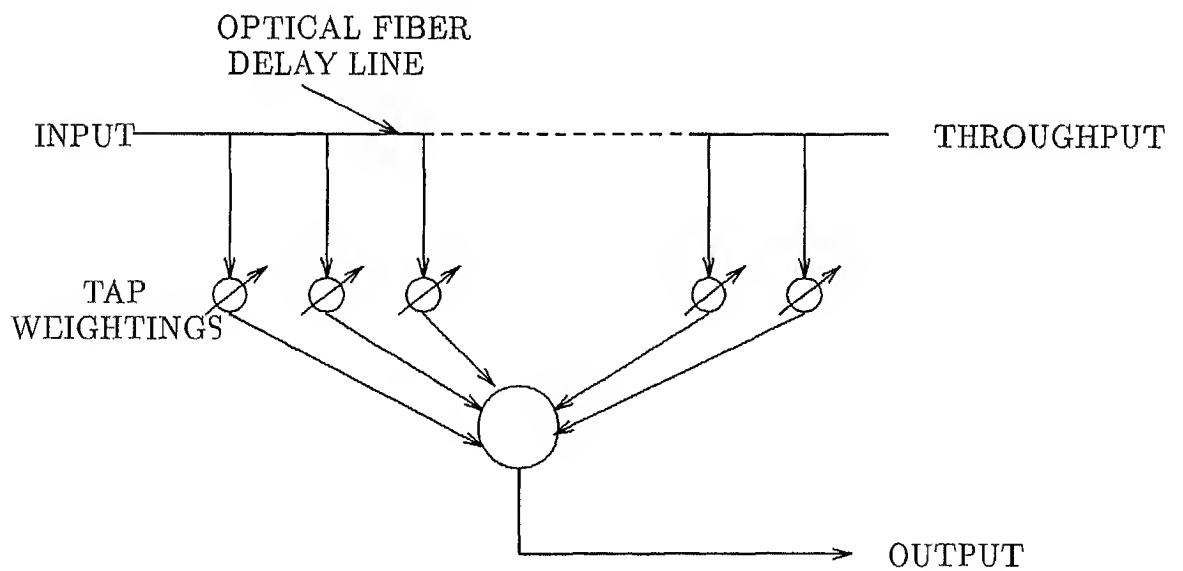


Figure 1.2 Tapped delay Line

is that it can not be used as a finite impulse response filter (FIR). The tapped delay line structure consists of a fiber with taps distributed along its length. Signals introduced into one end are successively sampled, weighted and then summed up either by optical summation before detection or by electronic summation after detection. A tapped delay line can be fabricated by putting a series of reflective mirrors [11] or a series of directional couplers [12] along the length of the fiber. Implementation of tapped delay lines using integrated optical architectures is considered in [13]. A tapped delay line can also be fabricated by creating a bundle of fiber strands of various lengths. One way to implement a fiber bundle based processor is to use two integrated optic fiber couplers [fig 1 3], one as a splitter at the input end and other as a combiner at the output. In another approach [fig 1 4], the fibers are tied up at the input end. The light outputs from the individual fibers are detected at the same detecting area by keeping a focusing arrangement in between the fiber outputs and the detector. This approach has the limitations in terms of maximum numbers of taps that can be obtained, due to the difficulties of uniformly illuminating and detecting light from a large number of bundled fibers. Still this method is attractive because of its low cost and the ease with which it can be implemented.

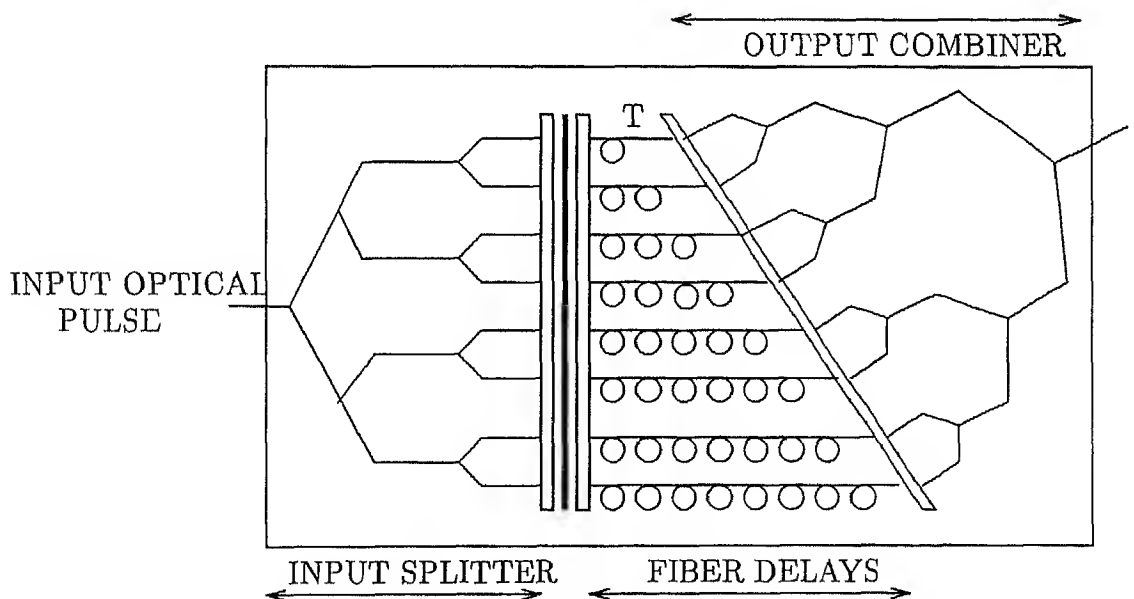


Figure 1 3 FIR fiber filter composed of input splitter and output combiner

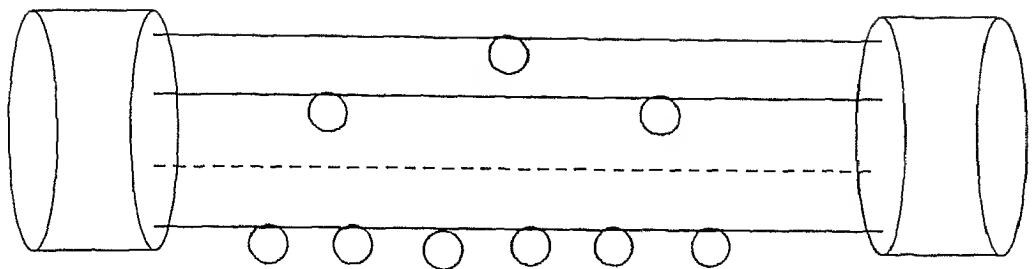


Figure 1 4 Fiber bundle approach

1 3 Objective of the present work

In this thesis, we discuss the design of a fiber bundle based transversal filter, which can be used as an equalizing filter in communication system in order to combat signal distortion. We have implemented a low pass filter with a cutoff frequency of 4.5 MHz. Seven fibers of appropriate lengths are chosen and all the tap weights are taken to be unity. The frequency response of the filter is calculated considering the effects of nonuniform coupling of light (between source and fibers and between fibers and detector) and bending losses of fiber. Coupling losses and bending losses are experimentally measured. The measured frequency response of the filter is compared with the calculated one and found to be in good agreement.

1 4 Overview

The basic design of a fiber optic transversal filter is discussed in chapter 2. The causes of non ideal response and their effects are considered in chapter 3. In the same chapter, the experimental part is considered in detail. In chapter 4 some applications of the fiber optic filter based on fiber bundle approach are discussed. Conclusion of the work along with some aspects of packaging is mentioned in chapter 5.

Chapter 2

Transversal Filters

Transversal filters offer a close approximation to any desired amplitude response with either no phase distortion at all or with a phase response that varies slowly and steadily regardless of the amplitude response [14]. A finite impulse response (FIR) filter used widely in Digital Signal Processing (DSP) is basically a transversal filter. A transversal filter consists of a series of delay sections to which signal is fed at one end and the signal is tapped after each delay. The tapped outputs are passed through gains and summed up to get the final output. The schematic of the filter is shown in the figure below.

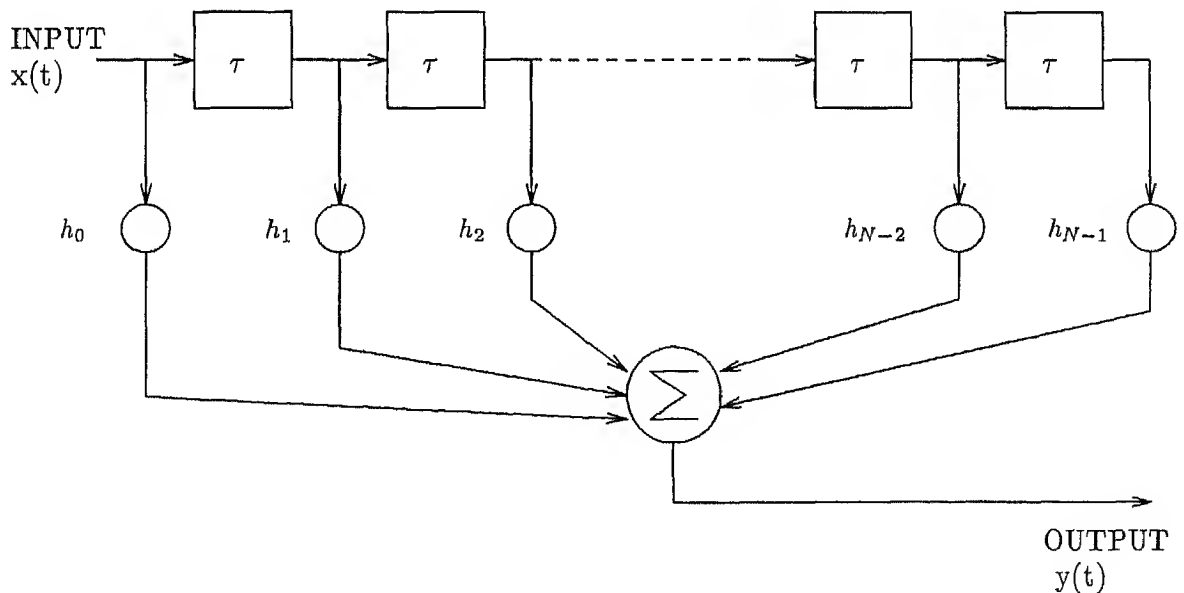


Figure 2.1 Transversal filter structure

The above structure contains $(N - 1)$ delay sections, each providing a delay of amount

τ and performs N multiplications and an addition. Clearly the relationship between input $x(t)$ and output $y(t)$ is given by,

$$y(t) = \sum_{i=0}^{N-1} h_i x(t - i\tau) \quad (21)$$

where, h_i is the tap weight and τ is the delay corresponding to one delay block

2.1 Fiber optic transversal filter

In this project, we design a fiber optic low pass filter of bandwidth of 4.5 MHz. We follow the bundled fiber approach. Fibers of different lengths are used to achieve different amount of delays.

The transversal filter with equal tap spacings consists of a group of fibers cut to lengths $l, l+L, \dots, l+(N-1)L$, where l is the length of the shortest fiber (also called as basic length), L is the length difference between two successive fibers and N is the total number of fibers. From eqn 2.1

$$y(t) = \sum_{i=0}^{N-1} h_i x(t - t_0 - i\tau) \quad (22)$$

where,

- $t_0 = n_g l / c$ = delay corresponding to the basic length,
- $\tau = n_g L / c$ = delay difference,
- n_g is refractive index of the material of fiber core, and
- c is velocity of the light in free space

Taking Fourier Transform of both sides of eqn 2.2, we get

$$Y(f) = \sum_{i=0}^{N-1} h_i e^{-j2\pi f(t_0 + i\tau)} X(f)$$

Thus, the transfer function of the filter is

$$H(f) = \frac{Y(f)}{X(f)} = \sum_{i=0}^{N-1} h_i e^{-j2\pi f(t_0 + i\tau)} \quad (23)$$

So, for all $h_i = 1$ the magnitude response of the filter is given by

$$|H(f)| = \left| \sum_{i=0}^{N-1} e^{-j2\pi f i \tau} \right| \quad (24)$$

2 2 Calculation of lengths

From eqn 2 3 we see that the frequency response of the transversal filter depends on three parameters These are,

- 1 Number of fibers, N
- 2 Length difference, L
- 3 weights, h_i 's

It should be noted here that the basic length, l , does not contribute to the magnitude response and hence theoretically is not constrained to any factor other than the loss that is associated with it For a fiber with loss coefficient of 3 7 dB/m we can choose the value for l to be equal to 100 cm, which can be cut with good accuracy and at the same time will not contribute any significant amount of loss In our case we have chosen all the weights (h_i 's) to be unity Hence from eqn 2 4

$$\begin{aligned} |H(f)| &= \left| \sum_{i=0}^{N-1} e^{-i2\pi f} \right| \\ &= \left| \frac{\sin(\pi f N\tau)}{\sin(\pi f\tau)} \right| \end{aligned} \quad (2 5)$$

Clearly, the maximum amplitude is N which occurs at $f=m/\tau$ $m=0, 1, \dots$ The minima

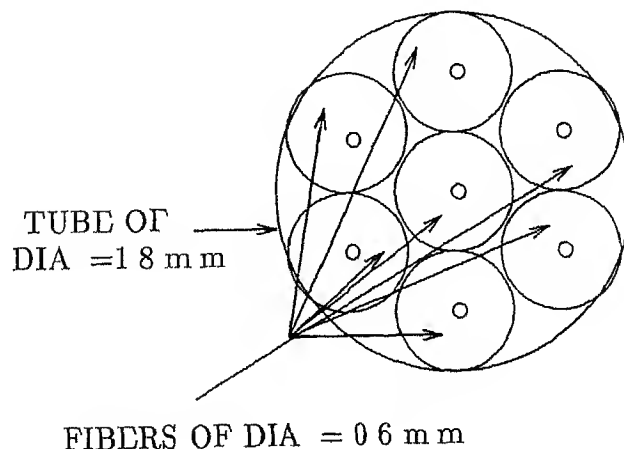


Figure 2 2 Cross sectional view of the fiber bundle at the ends

at which $|H(f)|$ is zero, are at $f=n/N\tau$, $n=1, 2, \dots$

Considering the problem of uniformly illuminating the fibers and detecting their outputs with a single detector, we have selected the value of $N = 7$. Selecting such a value of N has the advantage that we can position six fibers symmetrically around the seventh fiber (cross sectional view of the arrangement is shown in fig 2.2) so that all the outer fibers will receive equal amount of power when the light source is Lambertian in nature and the central fiber is perfectly aligned with the source to receive the peak amount of power.

The value of τ can be determined if one specifies the frequency where the first minimum occurs. We have taken it to be 10.105 MHz considering the availability of the driver and receiver circuits. So $\frac{1}{7\tau} = 10.105 \text{ MHz}$. Hence

$$\begin{aligned} L &= c\tau/n_g \\ &= 282.74 \text{ cm} \end{aligned}$$

$$[n_g = 1.5 \quad c = 3 \times 10^8 \text{ m/sec}]$$

Hence the lengths of the fibers are 1 m, 3.83 m, 6.66 m, 9.19 m, 12.32 m, 15.15 m, and

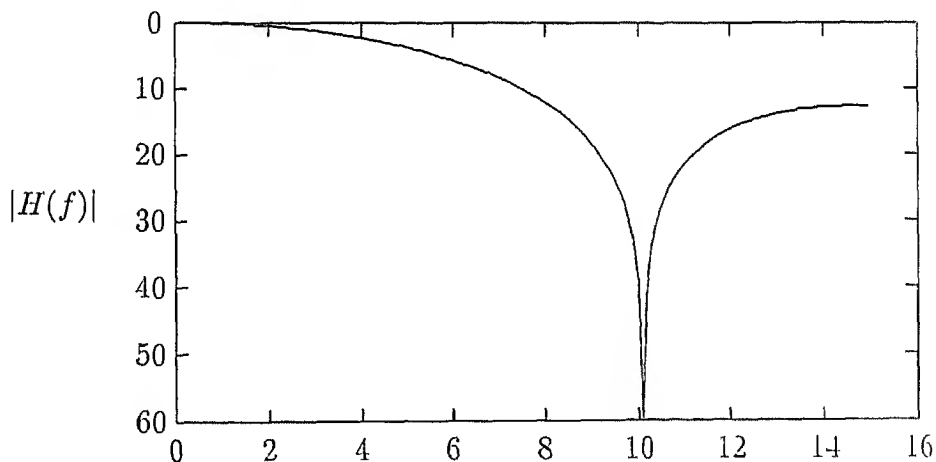


Figure 2.3 Ideal frequency response of the fiber optic filter

17.98 m

The plot of the magnitude response, taking the above value of $\tau = N = 7$ and all $h's = 1$ is shown in the attached graph (fig 2.3). The 3 dB passband width is 4.5 MHz.

Chapter 3

Experiment And Discussions

In this chapter we discuss the details of the experiment to measure the frequency response of the fiber optic transversal filter we designed in chapter 2. The perturbing factors like non uniform coupling of light into the fibers in the bundle, bending loss and fiber loss bandwidth limitations of the driver and receiver circuits are considered to obtain the expected frequency response of the filter. We will discuss the experiment and the result obtained.

3.1 Experimental set up

The devices/instruments we have used to perform the experiment are,

- 1 FM/AM signal generator,
- 2 Oscilloscope,
- 3 Analog LED driver module,
- 4 Fiber optic analog receiver module,
- 5 Fiber bundle based transversal filter

The block diagram of the set up is as shown in fig 3.1

The FM/AM generator used is made by KIKUSUI (Model No KSG4 300). It covers the frequency range from 10 KHz to 280 MHz. It generates highly stable signal with the resolution of 100 Hz. The signal generator feeds an analog fiber optic transmitter. In the analog transmitter circuit, the light output of a LED (Part no MFOE71, fig 3.2) is intensity modulated. The wavelength of the light emitted by the LED is typically 820 nm.

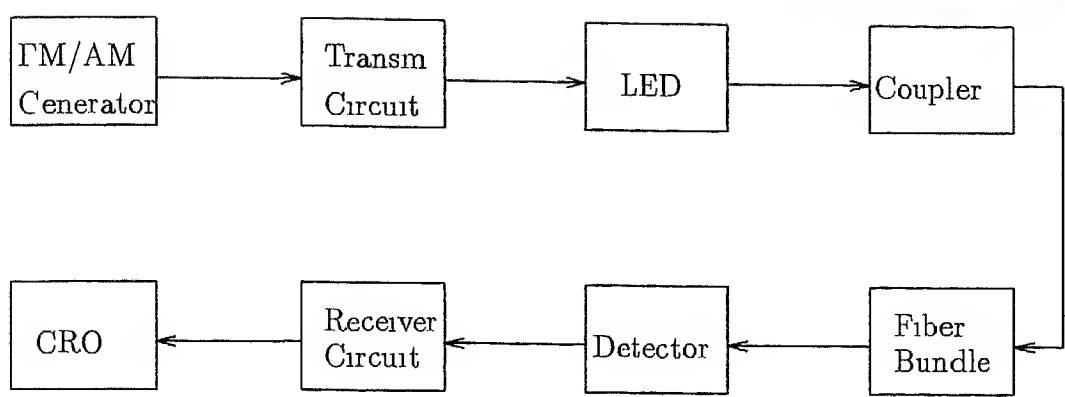


Figure 3 1 Experimental set up for measuring the frequency response of the fiber optic transversal filter

and the bandwidth is approximately 100 MHz LED is chosen as a light source since this is reasonably linear, thus generating light output that is almost linearly proportional to the drive current passing through it The responsivity of the photodetector (MFOD 71)

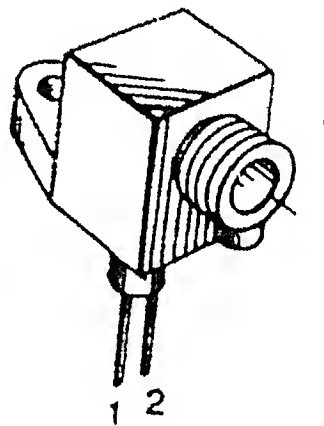


Figure 3 2 Light emitting diode, model MFOE71 [Ref]

that we used is typically $0.2 \mu\text{A}/\mu\text{W}$ at 820 nm wavelength

In the receiver module, transimpedance type configuration is chosen for the preamplifier stage This design yields both low noise and a large dynamic range The amplifier band width can be sufficiently increased to minimize distortion, and to do away with equalizer which is needed for high input impedance type front end The postamplifier used here consists of a integrated circuit differential video amplifier LM733 The transmitter and the receiver modules were developed earlier in our laboratory to use them in a fiber optic

analog link [15]

The oscilloscope is of bandwidth 40 MHz and made by KIKUSUI (Model No DSS 5040)

3 2 Fiber bundle preparation

Seven pieces of fiber of lengths 1 m 3 83 m, 6 66 m, 9 49 m, 12 32 m, 15 15 m, and 17 98 m are cut from the spool. A solid cylinder with a diameter of 15 cm is taken. Other than the first fiber all fibers are wrapped on the cylinder. With this choice of the cylinder dimension, the i th fiber needs to be wrapped to make $6(i-1)$ complete turns after which 100 cm of its length will be left out. The fibers are wound in a manner such that no two fibers overlap each other. The total no of loops is thus,

$$\sum_{i=1}^7 6(i-1) = 126$$

The height of the cylinder must be at least $126 \times 0.6 = 75.6$ mm as fiber diameter (with jacket) is 0.6 mm. The end faces of each of the fibers are prepared as follows

- 1 The sheathing of the fiber is exposed by stripping the plastic jacket by an amount of 8 cm
- 2 The exposed fiber is rubbed with a tissue paper with propanol until the glass is completely cleaned from plastic
- 3 The exposed fiber is scribed with a fiber cleaver at a distance of 7 cm from the end
- 4 The fiber is sliced in the opposite direction from the scribe mark. At the same time the fiber is pulled till it breaks

Ends of the fibers are tied up by using plastic tube of length 1.2 cm and of diameter 1.8 mm. The longest fiber is carefully positioned so that it remains at the central position of the bundle.

The same procedure is followed to prepare another bundle on a cylinder of diameter 10 cm. In this case the i th fiber needs to be wrapped by $9(i-1)$ complete loops and hence

the minimum value of the cylinder height should be

$$\left(\sum_{i=1}^7 9(i-1) \right) \times 0.6 = 113.4 \text{ mm}$$

3.3 Causes of non-ideal response and their effects

Referring to fig 3.1, the frequency response of the fiber optic filter is given by

$$H(f) = H_1(f)H_2(f)H_3(f)H_4(f) \quad (3.1)$$

where

- $H_1(f)$ is the frequency response of the fiber bundle including the coupling effect between adjacent fibers.
- $H_2(f)$ is the frequency response of the combined transmitter and receiver,
- $H_3(f)$ is the combined frequency response of the LED and Photodiode
- $H_4(f)$ is the combined frequency response of the FM/AM generator and CRO

The frequency response of the filter which was shown earlier in fig 2.3 is not practically achievable, because of the following factors. These are,

- 1 Non uniform coupling of light into fibers,
- 2 Bending loss,
- 3 Fiber loss,
- 4 Bandwidth limitations of the transmitter and receiver circuits,
- 5 Bandwidth limitations of the LED and Detector,
- 6 Bandwidth limitations of the measuring and testing instruments

Item 5 in the above list does not contribute to the frequency response of filter as the LED and the photodiode can be used upto 100 MHz, whereas our filter is designed to have a cutoff frequency of 10 MHz. Item 6, too, does not have any effect on the filter performance as the FM/AM generator can deliver stable oscillation upto 280 MHz and the oscilloscope, being used, has a bandwidth of 40 MHz.

The transmitter and the receiver do not have constant frequency response in the range of frequency from d c to 10 MHz and thus can affect the overall frequency response of the filter

To include the effects of the first three items in the above list, we can modify the transfer function in eqn 2.3 in the following way,

$$H_1(f) = \sum_{n=0}^{N-1} (1 + \delta_n) e^{-j2\pi f(\tau+n)} \quad (3.2)$$

where, δ represents the perturbation in the filter coefficients. We can consider δ to be composed of three parts. These are δ_{ic} , δ_{if} and δ_b arising from the non uniform coupling, fiber losses and bending losses respectively. We will now consider these effects in turn.

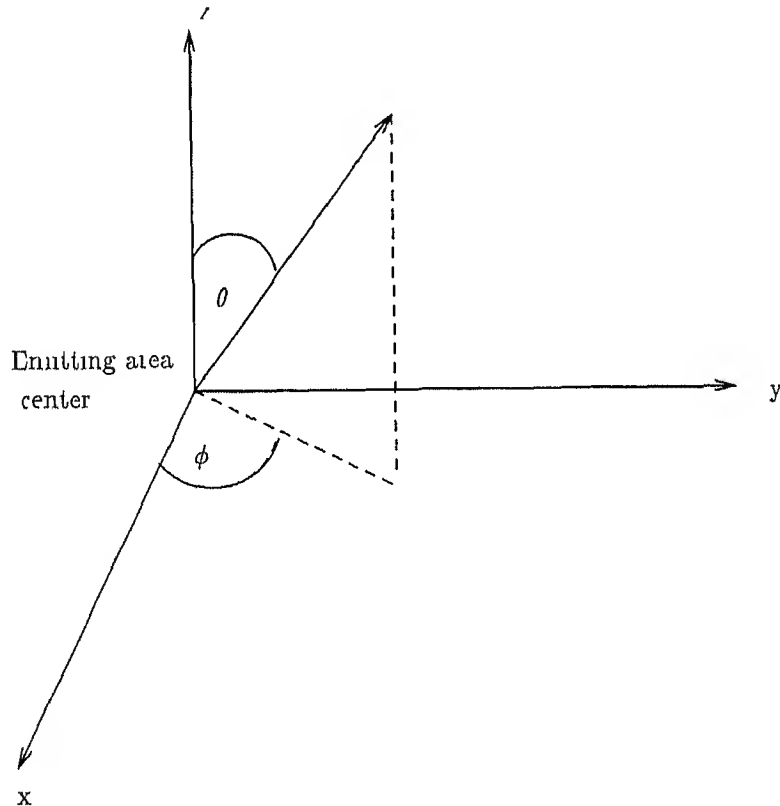


Figure 3.3 Spherical coordinate system

3.3.1 Non-uniform coupling effect

To achieve the ideal response of the filter, all the fibers in the fiber bundle delay line should be provided with equal amount of light power. Distributing the LED output power

uniformly among the fibers is a difficult task. Particularly in our case as we did not use any intermediate optics to collimate the LED light all the fibers do not receive same amount of power.

To determine the optical power accepting capability of a fiber the spatial radiation pattern of the LED must first be known. Let us look at fig 3.3 which shows a spherical coordinate system characterized by r , θ and ϕ . The irradiance of LED may be a function of both θ and ϕ . The emission pattern of a LED follows the relationship [18]

$$B(\theta) = B(0) \cos \theta \quad (3.3)$$

and

$$B(\phi) = B(0) \cos^n \phi \quad (3.4)$$

For the LED that we have used, the values of m and n are not available in the catalog. We have experimentally measured the far field pattern of the LED using the set up shown in fig 3.5. The LED is mounted on a printed circuit board (PCB). This PCB is fixed on the optical bench using a holder. LED is driven by a constant current of approximately 30 mA. The current is obtained (fig 3.4) by shorting all the inputs of a NAND gate to ground and connecting the high output of the NAND gate to the LED through a resistance of 100 Ω . With the help of another holder the detector is positioned on the optical bench at a distance of 12 cm from the LED. The detector is connected in series with a resistance of 100 K Ω and the voltage across the resistance is measured with a digital multimeter whose accuracy is 0.1 percent. The lateral, vertical and rotational knobs of the LED holder are adjusted to get the maximum output from the detector. The LED is now rotated with respect to the detector both in clockwise and anti clockwise direction and the detector output voltage is noted down (table 3.1). To obtain the radiation pattern in θ direction, the PCB containing the LED is rotated by 90 degree with respect to its initial position and the experiment is repeated. The readings (normalized) are shown in table 3.1. To find out the values for m and n , we have taken polar plots of eqn 3.3 and 3.4 for different values of m and n . The experimental data are also plotted and found to be closely matching with the patterns obtained by using,

$$\frac{B(\theta)}{B(0)} = \cos^{50} \theta$$

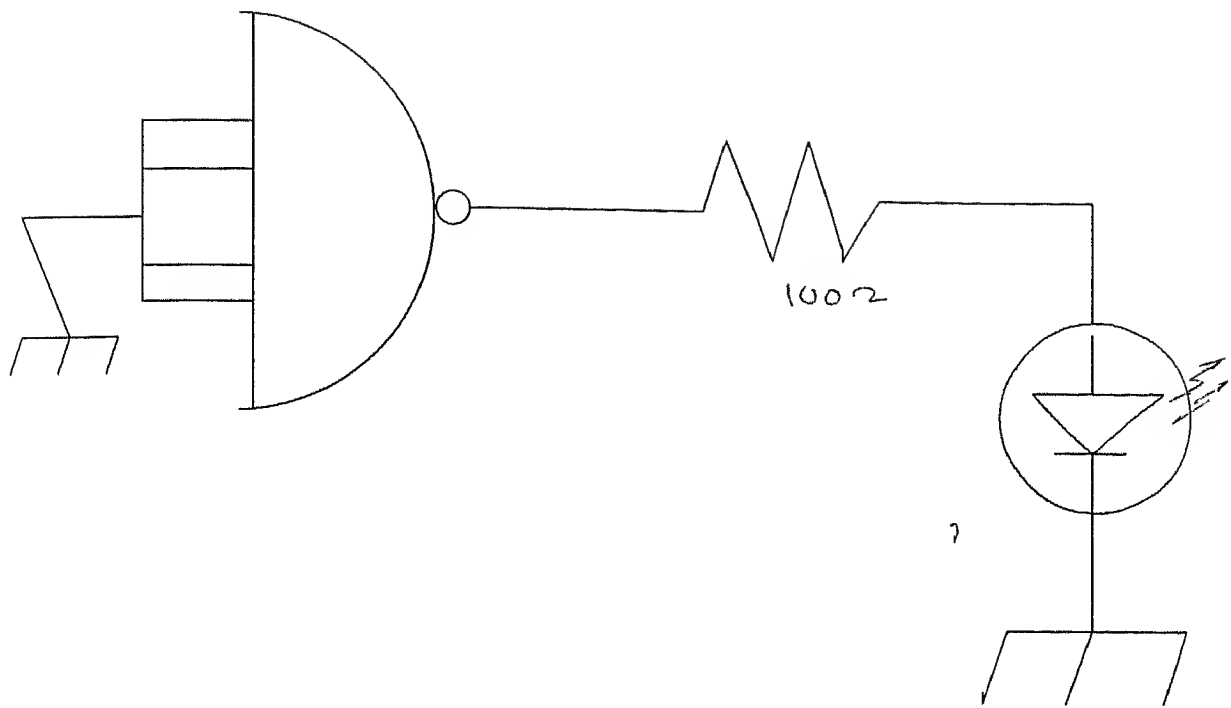


Figure 3.4 Driver circuit of the LED to measure the far field pattern

and

$$\frac{B(\phi)}{B(0)} = \cos^{50}\phi$$

In fig 3.6 we have plotted the experimental far field pattern of the LED in the ϕ direction, as well as the theoretical pattern for $m = 50$. They are seen to be matching very closely to each other. In fig 3.7, the experimental far field pattern in θ direction is compared with the theoretical one with $n = 50$ and once again they are very closely matched.

We have found here through our experiment of measuring far field pattern, the source radiation pattern is symmetric in nature as the values for m and n are equal. Hence, if the central fiber of the bundle is perfectly aligned so that it receives the peak amount of power, the other fibers, being symmetrically positioned with respect to the central fiber will receive equal amount of power among themselves. The fractional power that the outer fibers receive can be calculated by using eqn 3.3, eqn 3.4, and by measuring the distance in between the LED and the fiber bundle endface and the distance between the cores of two adjacent fibers. In fig 3.8, the dimensional details of the coupling between LED and the fiber bundle is shown. The distance between LED and the fiber bundle endface is taken to

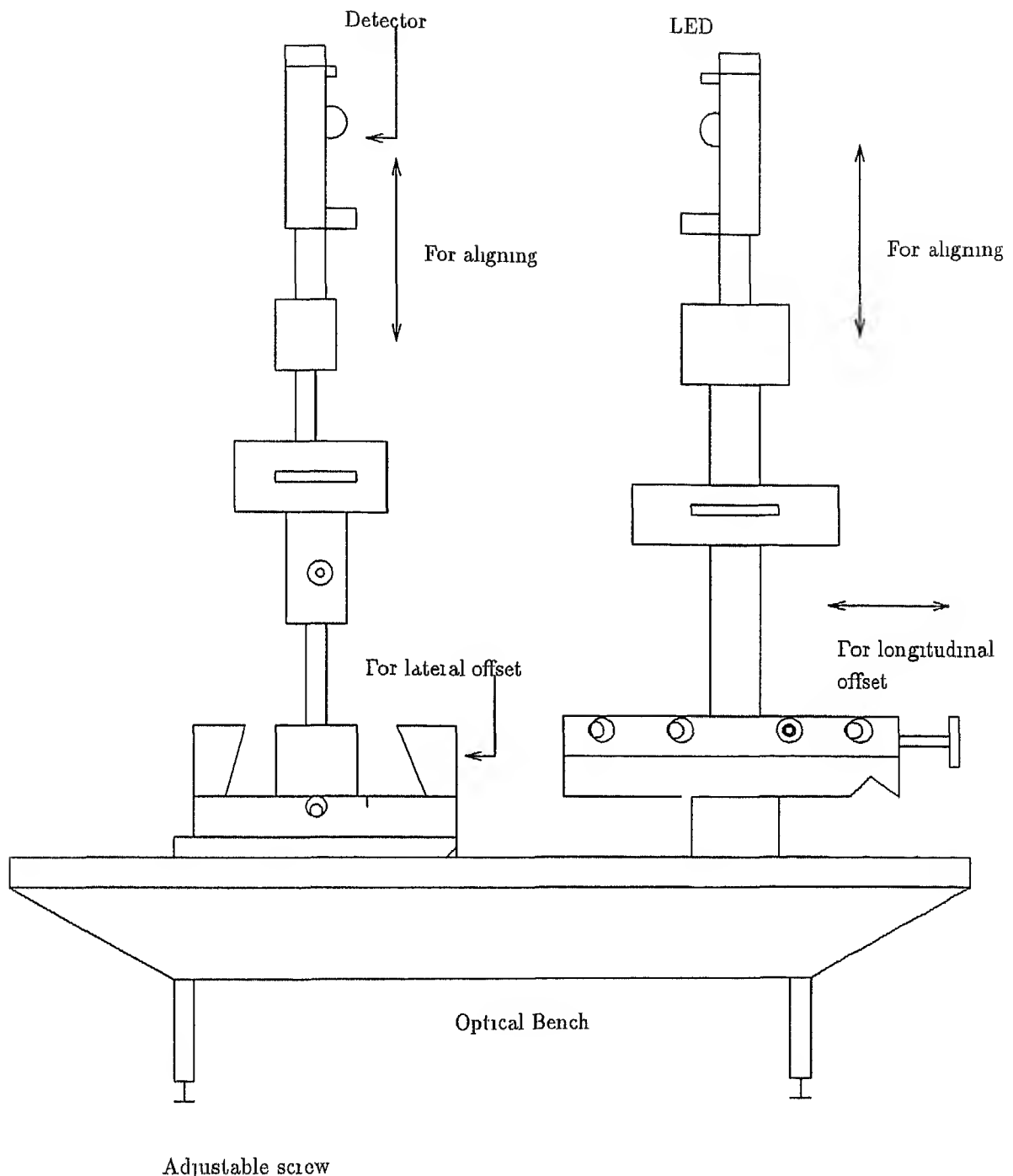


Figure 3.5 Experimental set up for measuring the far field pattern of the LED

Sl No	Angle in Degrees	Relative Intensity in ϕ Direction	Relative Intensity in θ Direction
1	90 to 35	0 105	0 138
2	30	0 108	0 138
3	25	0 110	0 140
4	20	0 124	0 171
5	18	0 145	0 206
6	16	0 174	0 248
7	14	0 220	0 276
8	12	0 253	0 348
9	10	0 367	0 515
10	9	0 524	0 580
11	8	0 618	0 610
12	7	0 695	0 680
13	6	0 761	0 779
14	5	0 825	0 828
15	4	0 881	0 881
16	3	0 925	0 911
17	2	0 944	0 971
18	1	0 983	0 997
19	0	1	1
20	1	0 980	0 984
21	2	0 943	0 969
22	3	0 923	0 935
23	4	0 881	0 877
24	5	0 824	0 812
25	6	0 761	0 719
26	7	0 690	0 682
27	8	0 609	0 621
28	9	0 511	0 578
29	10	0 360	0 510
30	12	0 250	0 349
31	14	0 219	0 278
32	16	0 179	0 249
33	18	0 142	0 214
34	20	0 120	0 172
35	25	0 107	0 140
36	30 to 90	0 105	0 137

Table 3.1 Far field radiation measurement data of LED

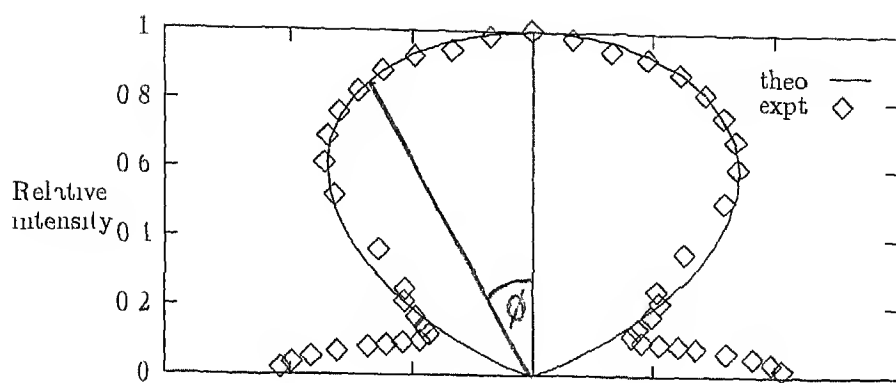


Figure 3.6 Far field pattern of LED in ϕ direction

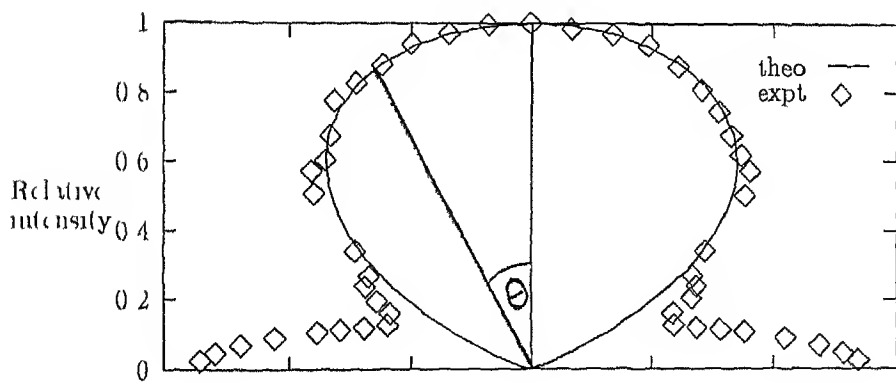


Figure 3.7 Far field pattern of LED in θ direction

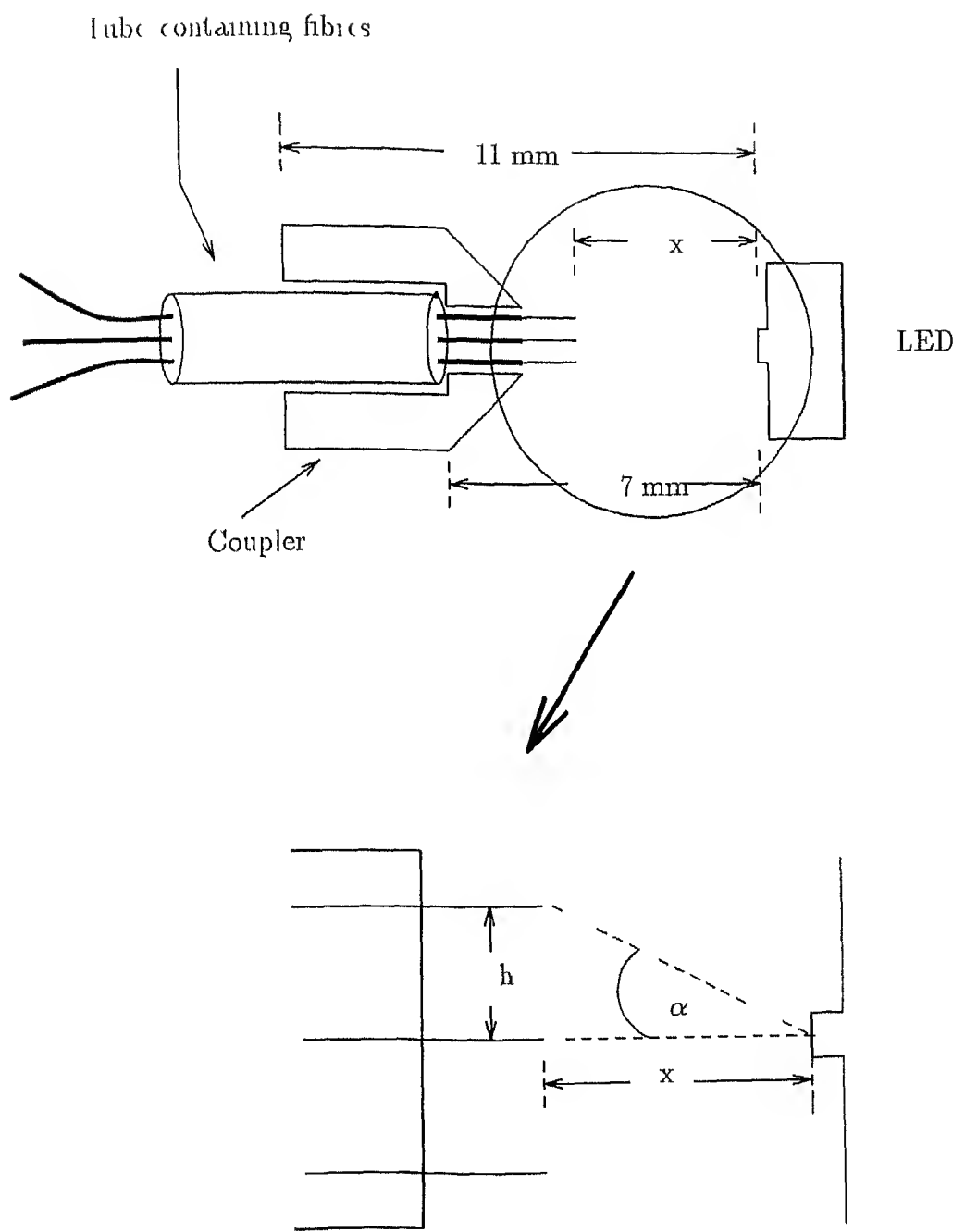


Figure 3.8 Inside dimensional details of coupling between LED and the fiber bundle

be τ . The core to core distance of two adjacent fibers is shown as h and it is measured to be 0.6 mm. We have considered three different values for x , which are 3 mm, 4 mm and 5 mm. Beyond 5 mm, the distance between the LED and the fiber bundle might be too large to couple sufficient amount of light to fibers. For distances less than 3 mm, outer fibers will receive much less amount of power with respect to the central fiber and hence, the non uniformity effect will be too high. The fractional power $f(h/x)$, is given by

$$f(h/\tau) = \cos^{-1} \left[\tan^{-1} \left(\frac{h}{x} \right) \right] \quad (3.5)$$

We used equation 3.5 to obtain the table 3.2, where the values of the fractional power is shown for three different values of τ .

Distance, x	Fractional power
3 mm	0.3751
4 mm	0.5734
5 mm	0.6995

Table 3.2 Fractional powers for different values of x

When we are considering the effect of non uniform illumination alone on the frequency response of the filter, δ_i in eqn 3.2 becomes equal to δ_{ic} . Weights get modified because of the perturbation term δ_{ic} in a way such that for $i=1$ to 6, $\delta_i + 1 = f(h/x)$, and for $i=7$, $\delta_i + 1 = 1$, considering all h_i 's to be 1 as in our case study. With the help of table 3.2, we can form table 3.3, which shows the values for δ_{ic} for different values of x . In fig 3.9, we show the effect of non uniform coupling on the frequency response of

Distance, x	$\delta_{ic}, i=1$ to 6	$\delta_{ic}, i=7$
3 mm	0.5249	0
4 mm	0.4266	0
5 mm	0.3005	0

Table 3.3 Values of δ_{ic} for different x

the filter. The frequency response corresponding to $x=5$ mm deviates less from the ideal frequency response than the frequency response corresponding to $x=3$ mm. We see that

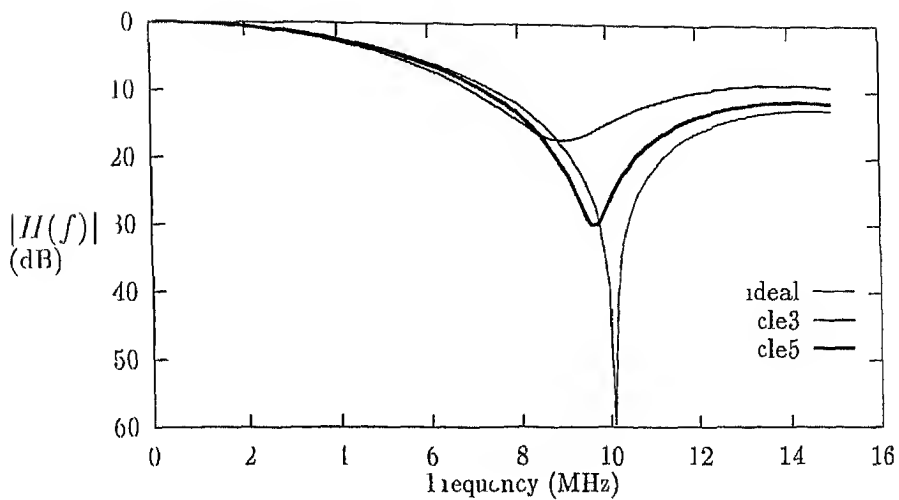


Figure 3.9 Coupling loss effect on the frequency response of the filter (cle3 is the response when $x=3$ mm, cle5 is the response when $x=5$ mm)

frequency response considering non uniform coupling effect has greater sidelobe than the ideal frequency response

3.3.2 Bending loss and fiber attenuation effect

As the fibers are wrapped on a cylindrical drum by different amounts, the bending loss will be different from fiber to fiber. Moreover, due to their differences in length, the signals will undergo different amount of losses when propagating through the fibers.

Bending loss

Radiative losses occur whenever an optical fiber undergoes a bend of a finite radius of curvature. In multimode fiber, since higher order modes are bound less tightly [16] to the fiber core than the lower order modes, the higher order modes will radiate out of the fiber first. Though the number of modes that are guided by a curved fiber can be found [17], unless the source excitation field is known explicitly, this can not be applied to find out the bending loss. Because of this limitation in using the formula mentioned in [17], we prefer to measure the bending loss. The experimental set up used is same as that mentioned in

the case of source output pattern measurement in the previous section. However in this case one 18 m long fiber is connected in between the LED and photodiode. This fiber is wrapped on a cylindrical drum of diameter 15 cm for $6N$ turns (N is an integer) and the detected output is measured and compared with the output obtained when there was no turn. The result of bending loss measurement is shown in table 3.4. The experiment is repeated by taking the cylinder of diameter 10 cm and in this case the number of

No of loops	P_{out}/P_n
0	1
6	0.998
12	0.997
18	0.997
21	0.995
30	0.994
36	0.991

Table 3.4 Bending loss measurement for diameter of curvature = 15 cm

No of loops	P_{out}/P
0	1
9	0.991
18	0.986
27	0.983
36	0.981
45	0.980
54	0.980

Table 3.5 Bending loss measurement for diameter of curvature = 10 cm

turns were multiples of 9. The bending loss data for 10 cm case are shown in table 3.5. Comparing the bending loss entries for 18 and 36 loops in tables 3.4 and 3.5 we see that losses for diameter of 10 cm is more than those for 15 cm diameter. Also the 18th fiber wrapped on a cylinder of 10 cm diameter suffers from larger bending loss than when it is wrapped on a cylinder of 15 cm diameter. The particular choices of cylinder dimension are taken, as we have implemented the fiber optic filter using these dimensions.

To consider the effect of bending loss alone on the frequency response of the filter δ ,

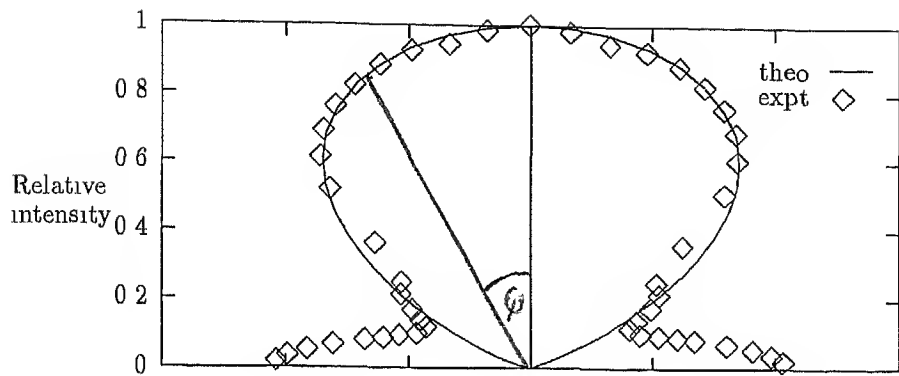


Figure 3.6 Far field pattern of LED in ϕ direction

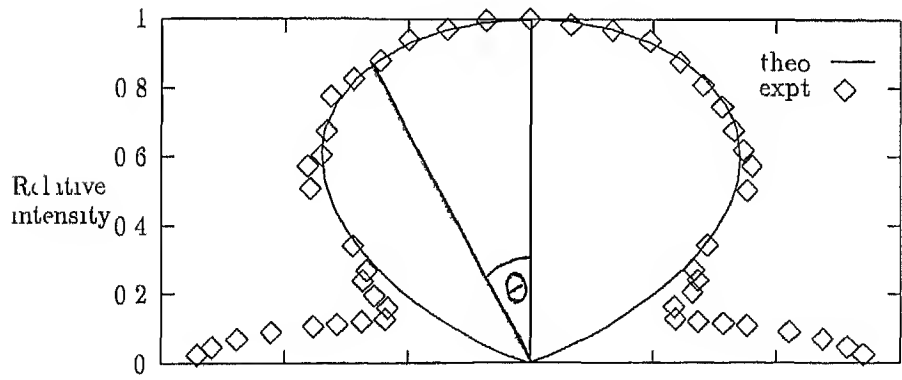


Figure 3.7 Far field pattern of LED in θ direction

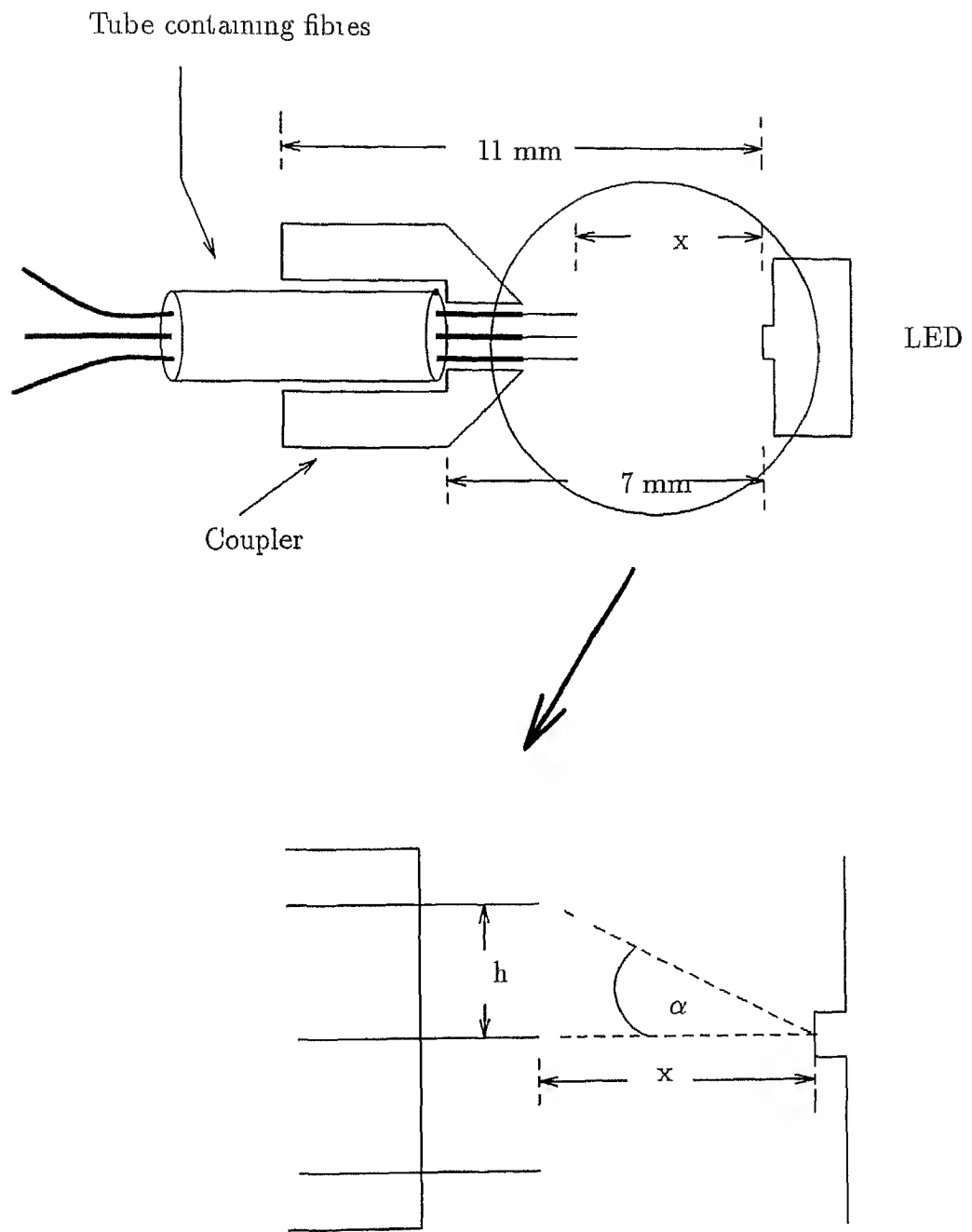


Figure 3.8 Inside dimensional details of coupling between LED and the fiber bundle

be r . The core to core distance of two adjacent fibers is shown as h and it is measured to be 0.6 mm. We have considered three different values for x , which are 3 mm, 4 mm and 5 mm. Beyond 5 mm the distance between the LED and the fiber bundle might be too large to couple sufficient amount of light to fibers. For distances less than 3 mm, outer fibers will receive much less amount of power with respect to the central fiber and hence, the non uniformity effect will be too high. The fractional power $f(h, x)$ is given by

$$f(h, x) = \cos^{50}[\tan^{-1}(\frac{h}{x})] \quad (3.5)$$

We used equation 3.5 to obtain the table 3.2, where the values of the fractional power is shown for three different values of x .

Distance, x	fractional power
3 mm	0.3751
4 mm	0.5734
5 mm	0.6995

Table 3.2 Fractional powers for different values of x

When we are considering the effect of non uniform illumination alone on the frequency response of the filter, δ_i in eqn 3.2 becomes equal to δ_{ic} . Weights get modified because of the perturbation term δ_{ic} in a way such that for $i=1$ to 6, $\delta_i + 1 = f(h, x)$, and for $i=7$, $\delta_{ic} + 1 = 1$, considering all h_i 's to be 1 as in our case study. With the help of table 3.2, we can form table 3.3, which shows the values for δ_{ic} for different values of x . In fig 3.9, we show the effect of non uniform coupling on the frequency response of

Distance, x	δ_i , $i=1$ to 6	δ_{ic} , $i=7$
3 mm	0.5249	0
4 mm	0.4266	0
5 mm	0.3005	0

Table 3.3 Values of δ_{ic} for different x

the filter. The frequency response corresponding to $x=5$ mm deviates less from the ideal frequency response than the frequency response corresponding to $x=3$ mm. We see that

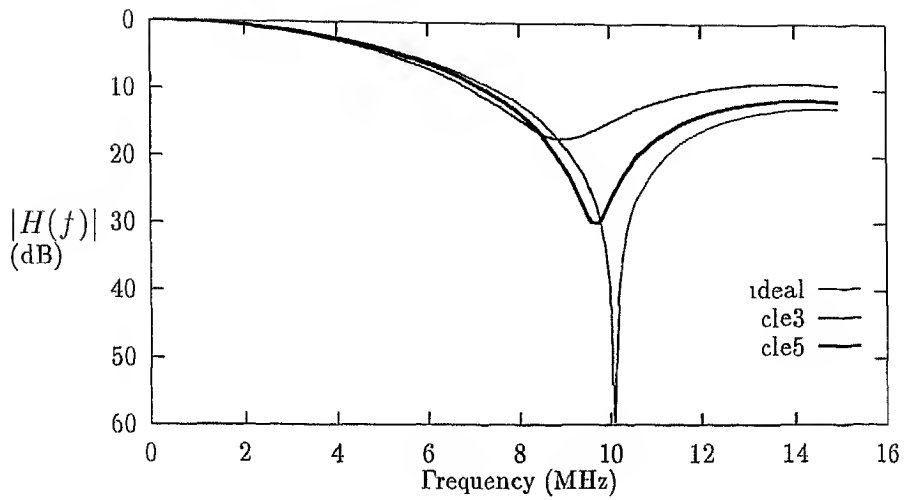


Figure 3.9 Coupling loss effect on the frequency response of the filter (cle3 is the response when $x=3$ mm, cle5 is the response when $x=5$ mm)

frequency response considering non uniform coupling effect has greater sidelobe than the ideal frequency response

3.3.2 Bending loss and fiber attenuation effect

As the fibers are wrapped on a cylindrical drum by different amounts, the bending loss will be different from fiber to fiber. Moreover, due to their differences in length, the signals will undergo different amount of losses when propagating through the fibers.

Bending loss

Radiative losses occur whenever an optical fiber undergoes a bend of a finite radius of curvature. In multimode fiber, since higher order modes are bound less tightly [16] to the fiber core than the lower order modes, the higher order modes will radiate out of the fiber first. Though the number of modes that are guided by a curved fiber can be found [17] unless the source excitation field is known explicitly, this can not be applied to find out the bending loss. Because of this limitation in using the formula mentioned in [17], we prefer to measure the bending loss. The experimental set up used is same as that mentioned in

the case of source output pattern measurement in the previous section. However in this case one 18 m long fiber is connected in between the LED and photodiode. This fiber is wrapped on a cylindrical drum of diameter 15 cm for $6N$ turns (N is an integer) and the detected output is measured and compared with the output obtained when there was no turn. The result of bending loss measurement is shown in table 3.4. The experiment is repeated by taking the cylinder of diameter 10 cm and in this case the number of

No of loops	P_{out}/P_n
0	1
6	0.998
12	0.997
18	0.997
24	0.995
30	0.994
36	0.991

Table 3.4 Bending loss measurement for diameter of curvature = 15 cm

No of loops	P_{out}/P_n
0	1
9	0.991
18	0.986
27	0.983
36	0.981
45	0.980
54	0.980

Table 3.5 Bending loss measurement for diameter of curvature = 10 cm

turns were multiples of 9. The bending loss data for 10 cm case are shown in table 3.5. Comparing the bending loss entries for 18 and 36 loops in tables 3.4 and 3.5 we see that losses for diameter of 10 cm is more than those for 15 cm diameter. Also the 18th fiber wrapped on a cylinder of 10 cm diameter suffers from larger bending loss than when it is wrapped on a cylinder of 15 cm diameter. The particular choices of cylinder dimension are taken, as we have implemented the fiber optic filter using these dimensions.

To consider the effect of bending loss alone on the frequency response of the filter δ ,

in eqn 3.1 will be equal to δ_b . Weights get modified because of the perturbation term δ_b in a way such that $\delta_{ib} + 1 = P_i/P_n$. Values of δ_{ib} for $i = 1$ to 7 and for bend diameters 10 and 15 cm are shown in table 3.6. Bending loss effect on the frequency response of

i	δ_{ib} for loop dia=15 cm	δ_b loop dia=10 cm
1	0	0
2	0.002	0.010
3	0.003	0.014
4	0.003	0.017
5	0.005	0.019
6	0.007	0.020
7	0.006	0.020

Table 3.6 Values of δ_b

the filter is shown in fig 3.10 which is for bend diameter = 10 cm and in fig 3.11 for bend diameter = 15 cm. We see from table 3.6 and figures 3.10 and 3.11 that large bends of 15 or 10 cm diameter cause no significant change in the frequency response of the filter.

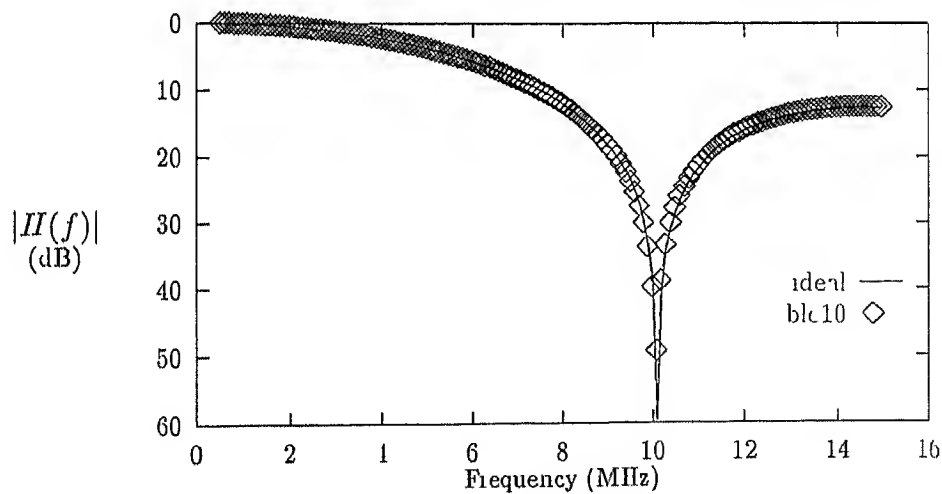


Figure 3.10 Bending loss effect on filter frequency response, loop dia=10 cm (blk10 is the response considering the bending loss)

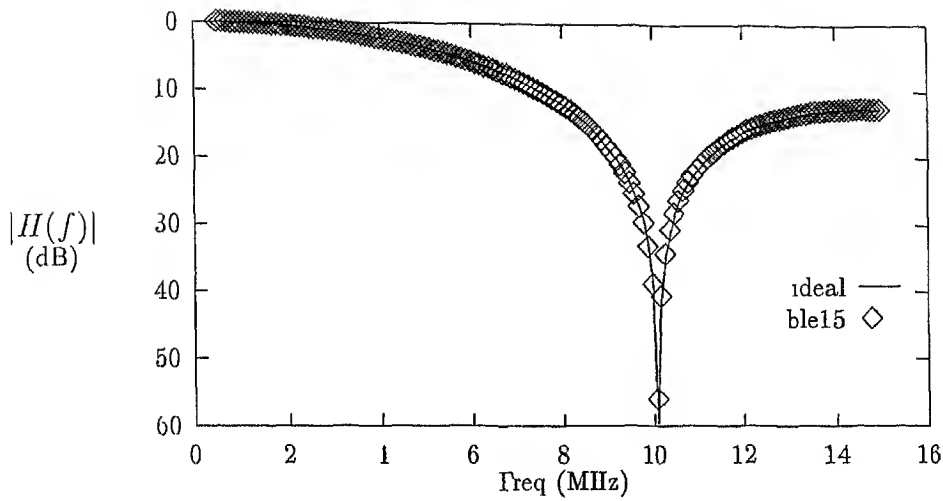


Figure 3.11 Bending loss effect on filter frequency response, loop of dia=15 cm (ble15 is the response considering the bending loss)

3.3.3 Attenuations of signal due to fiber loss

The fibers, we used here, has an attenuation coefficients of 3.7 dB/km at 820 nm of wavelength. With this coefficient, the loss for the i th fiber of length $(283i - 183)$ cm is

$$(283i - 183) \times (3.7 \times 10^{-3})$$

Using the expression of fiber loss as given above, losses for all the 7 fibers are calculated and the weights of the filters are modified according to equation 3.2. When only fiber loss is taken into account we get,

$$\begin{aligned} \delta_i &= \delta_f \\ &= 10^{[(283i - 183) \times (3.7 \times 10^{-3})]} - 1 \end{aligned} \quad (3.6)$$

which is negligible

3.3.4 Transmitter and Receiver circuits bandwidth limitations

The frequency response of the LED driver circuit and the receiver circuit is measured together. The transmitter circuit is driven by sinusoidal signals of varying frequency between

500 KHz to 10 MHz. The receiver output is measured with the help of a CRO. The link between the LED and the detector is a plastic fiber of length 100 cm. The frequency response $H_2(f)$ of the combined transmitter and the receiver circuit is shown in the fig 3.12 and the 3 dB cutoff frequency is found to be 8.4 MHz. As the response is not constant throughout the range upto 10 MHz, the transmitter and the receiver circuit affects the fre

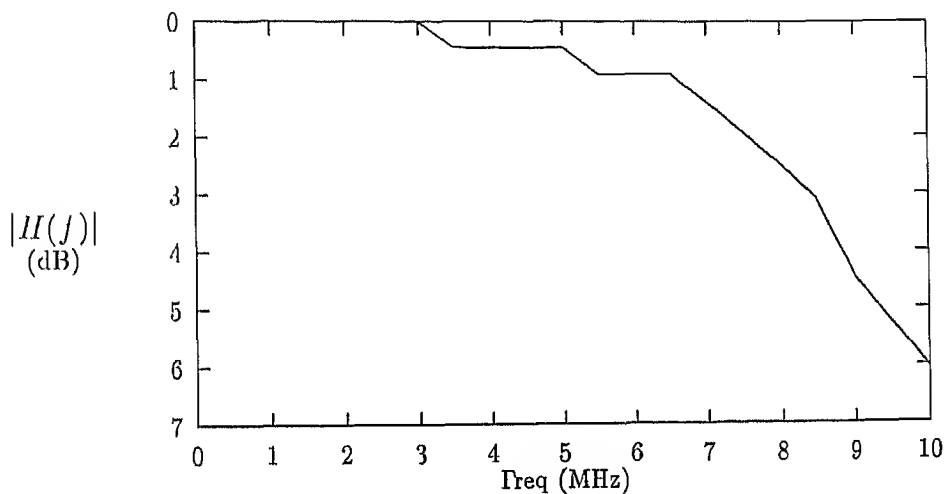


Figure 3.12 Combined frequency response of transmitter and receiver circuit

quency response of one fiber optic lowpass filter. This effect is shown in fig 3.13 and we see that it alters the filter frequency response by a significant amount. 3 dB bandwidth of the frequency response considering the transmitter and receiver circuit bandwidth limitations is seen to be changed to 4.2 MHz from 4.5 MHz for ideal frequency response. These two frequency responses differ by a maximum amount of 5.98 dB at frequency 10 MHz. After examining the effects of non uniform illumination, bending loss, fiber attenuation and the bandwidth limitations of the transmitter and receiver circuits individually on the frequency response of the filter, we have combined them all. The coefficients of the ideal filters are modified according to eqn 3.2 to consider the effects of non uniform illumination, bending loss and fiber loss. The transfer function of the filter obtained is then multiplied with the transfer function $H_2(f)$. The resulting filter frequency response is shown in fig 3.14 and in 3.15. In fig 3.14, we have considered the case when the loop diameter is 10 cm and the

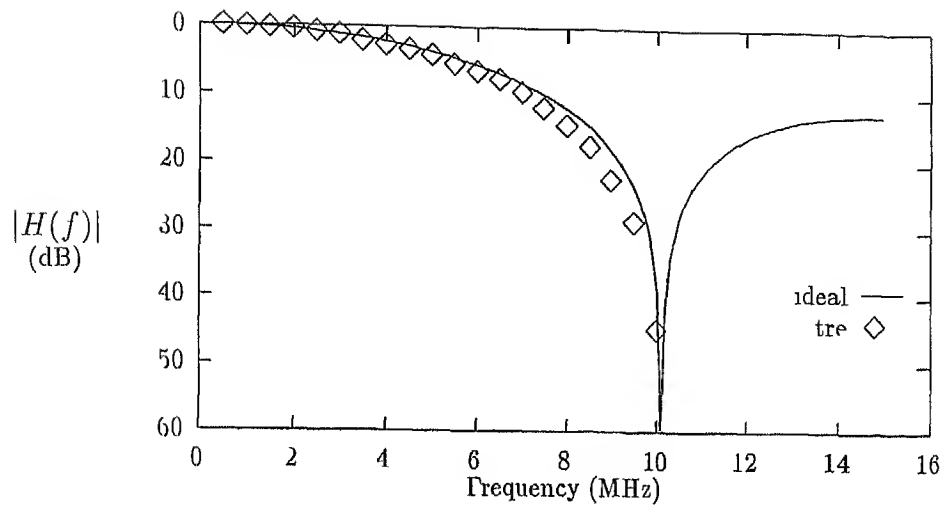


Figure 3.13 Transmitter and Receiver effect on frequency response (tre is the response considering the transmitter and receiver effect)

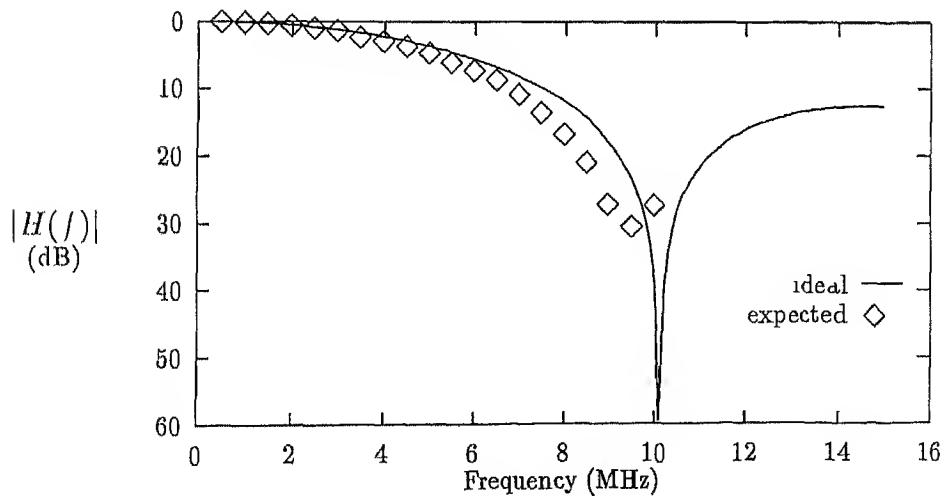


Figure 3.14 Expected fiber optic filter frequency response, $d=10$ cm and $x=4$ mm

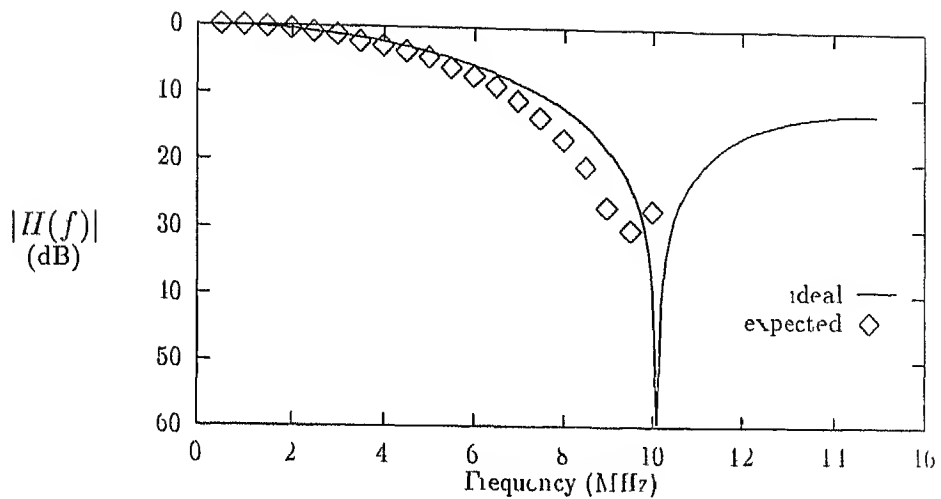


Figure 3.15 Expected fiber optic filter frequency response $d=15$ cm and $x=4$ mm

distance between the fiber bundle and the LED, x , is 4 mm whereas in fig 3.15 the diameter is changed to be 15 cm. Both the responses show a difference from the ideal frequency response.

3.4 Experimental Results

The experiment is done in two parts, one for the loop diameter of 15 cm and another for 10 cm.

In the first part of the experiment, altogether seven sets of readings are taken. In first three sets, the filter is tested for three different values of x , the distance between the light emitting diode and the corresponding fiber endface. In fig 3.16 the experimental data for $x=4$ mm is plotted and compared with the corresponding frequency response of the filter considering all the perturbing factors. Experimental curve is close to the theoretical curve. The other two measurements are taken by varying the distance between the LED and the fiber bundle endface. In one case, it is 3 mm and in another it is 1 mm. The results obtained match closely in both the cases and relative percentage error was always less than 20 percent. In last four measurements, we have implemented the idea of making some of the weights equal to zero, thereby changing the filter. It is accomplished by pulling

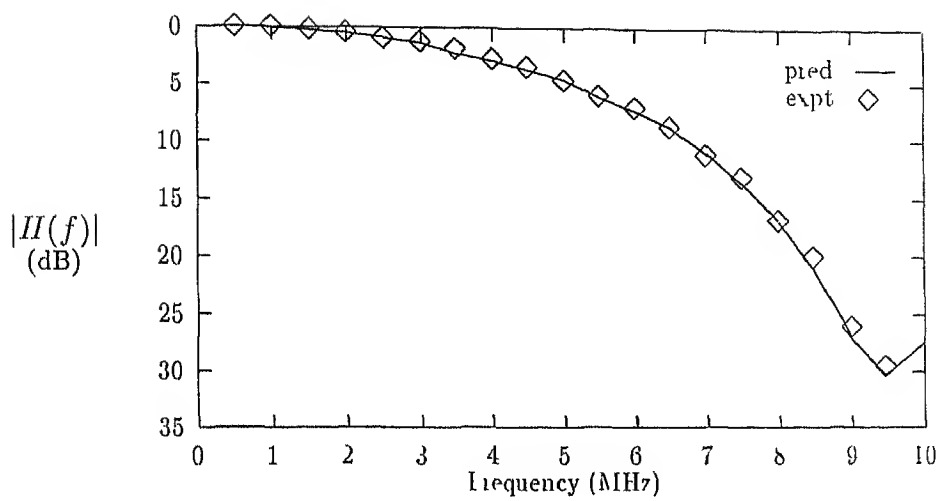


Figure 3.16 Comparison between the experimental plot with predicted one $d=15$ cm $x=4$ mm, all $h_i's=1$

out the respective fiber or fibers from the bundle at the detector side hence by blocking the corresponding light output from reaching to the detector To maintain the rigidity of the bundle, small pieces of fiber (approximately of 2 cm length) is substituted in place of the original fiber The experiment is repeated by blocking the second fiber fourth fiber sixth and second, fourth and sixth fibers together The experimental data are compared with the actual values and they are matching closely One curve is shown in fig 3.18 where we have measured the frequency response of the filter by taking out three fibers (fiber no 2, 4, and 6) from the bundle The other three measurements are taken by blocking the 2nd, 4th, and the 6th fiber one at a time and the experimental results are matching satisfactorily with the theoretical results

The second part of the experiment with a loop diameter of 10 cm is done in the same way as described earlier for 15 cm loop, with the difference that in this case we have blocked the fiber 3 , fiber 5, and fibers 3 and 5 together The results are shown for two measurements In fig 3.19, the distance between the fiber bundle and the LED is kept at 1 mm The experimental curve is very close to the theoretical one, as evident in the fig 3.19 Fig 3.20 shows the comparison between the experimental frequency response when 3rd and 5th

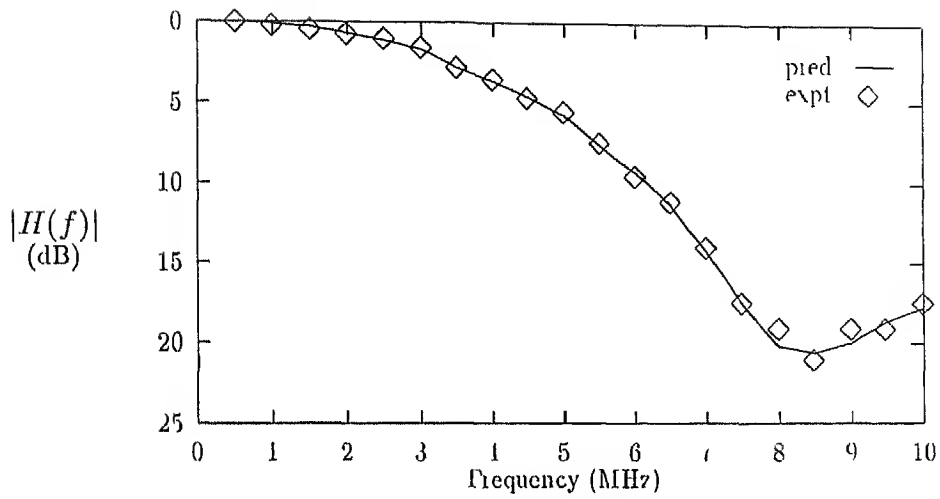


Figure 3.17 Comparison between the experimental plot with predicted one $d=15$ cm, $x=4$ mm, $h_2=h_4=h_c=0$, other h 's=1

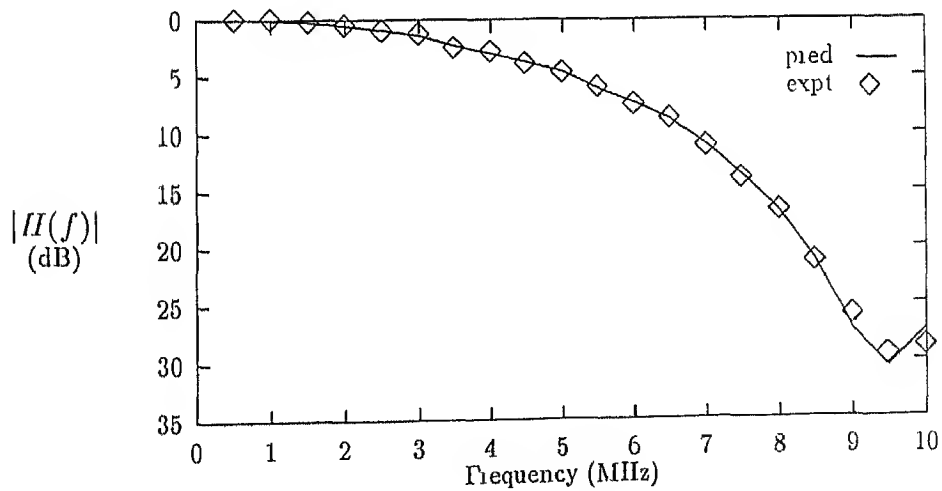


Figure 3.18 Comparison between the experimental plot with predicted one $d=10$ cm, $x=4$ mm, all h 's=1

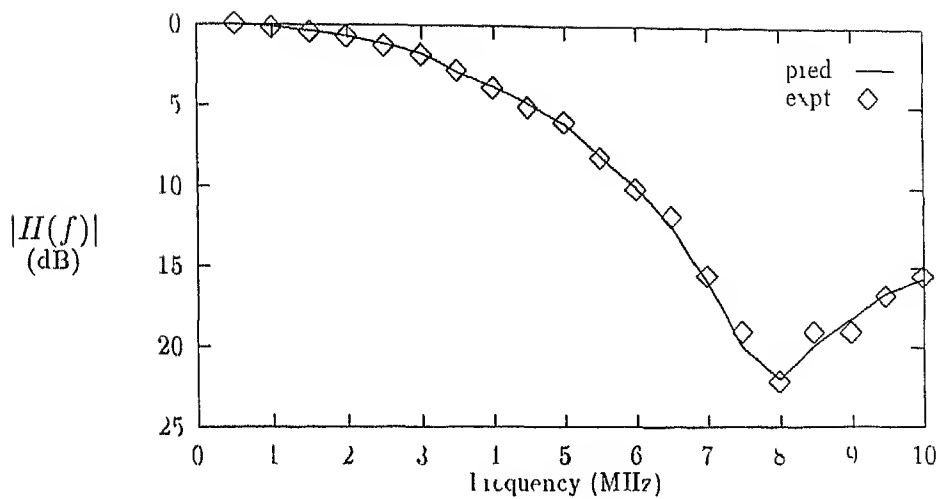


Figure 3.19 Comparison between the experimental plot with predicted one $d=10$ cm $x=4$ mm, $h_3=h_5=0$, other h_i 's=1

fibers are not there in the bundle

The experimental results show that it is possible to realize a fiber optic filter using the simple approach of fiber bundle technique. The closeness of the experimental frequency response with the expected one confirms the validity of the measurements taken in connection with the LED radiation pattern, bending loss and the transmitter receiver frequency response and also the validity of the subsequent discussion where these effects are taken into account to obtain the expected frequency response of the filter in figures 3.14 and 3.15

Chapter 4

Applications of fiber-optic tapped delay line devices

A fiber optic tapped delay line device can be used as a building block in several signal processing areas. Some of the applications of the fiber bundle tapped delay line are code generation, correlation and matched filtering, adaptive filtering and equalization, spread spectrum CDMA, spectral analysis of radio frequency signals, filtering with non uniform tap spacing etc. These applications are discussed briefly in the following sections.

4.1 Code generation and matched filtering application

The fiber optic tapped delay line can be used for code generation [7] by using a configuration shown in fig 4.1. An optical pulse $x(t)$ is injected into the device and a transmission mask is inserted so that individual tap outputs can be weighted by spatial filtering. The lens collects the transmitted tap light and images it onto a single photodetector. The output of the photodetector consists of a series of pulses whose timing corresponds to the length difference of the fibers in the bundle. By discretely weighting the taps with zeros and ones (i.e., blocking or transmitting the tap light at the image plane), the delay line can be used to generate any desired on off code at Gbit/s rates. The code generator can be made programmable using an electronically programmable liquid crystal array as the transmission mask.

This tapped delay line can also be used as a matched filter, where the transmission mask represents a reference code or sampled analog signal. When digital or analog optical

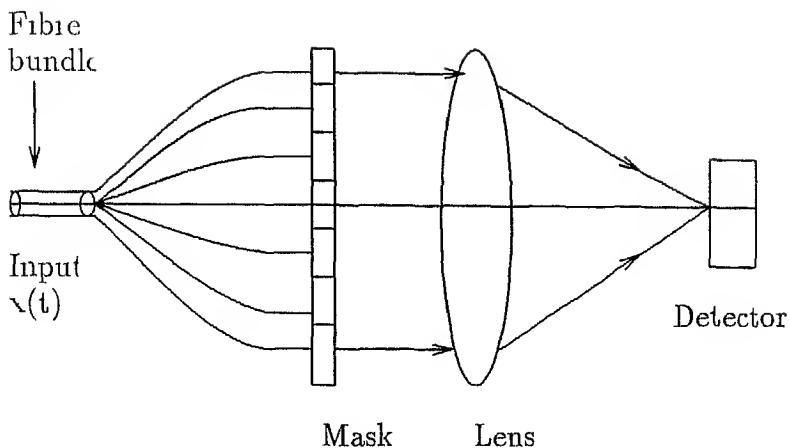


Figure 4.1 Block diagram of a fiber optic code generator

signal is inserted into the fiber, the output of the photodetector is the convolution of the propagating input signal with the fixed reference. If the input signal matches the reference, a strong correlation peak is observed. The design for both the code generator and the matched filter can be scaled for higher frequency by decreasing the length difference.

4.2 Fiber optic adaptive filters and equalizers

An adaptive processor has the ability to self optimize by continually monitoring its performance and updating its parameters. A general form of the tapped delay line adaptive filter or equalizer is shown in fig 4.2. The estimated signal is subtracted from the desired response and the residual signal is fed back to control the tap weights. An adaptive filter using least mean square algorithm for adjusting the weights is discussed in [19]. In fig 4.3, a fiber optic adaptive filter/equalizer using a bundle type fiber optic tapped delay line is shown. The signal $r(t)$ is divided equally in the $2N$ fiber strands for obtaining two sets of delayed samples X_n . For each element of X_n there are two strands of fibers of equal length. One half of the SLM mask is written with the values of the weight W_n , and the other half stores the error signal E_n . The vector multiplications are carried out as soon as light from the strands passes through the mask pixels and is collected by the detectors. The analysis for the convergence or learning characteristics of the adaptive filtering process as a function of the filter parameters and the fiber optic hardware errors are given in ref

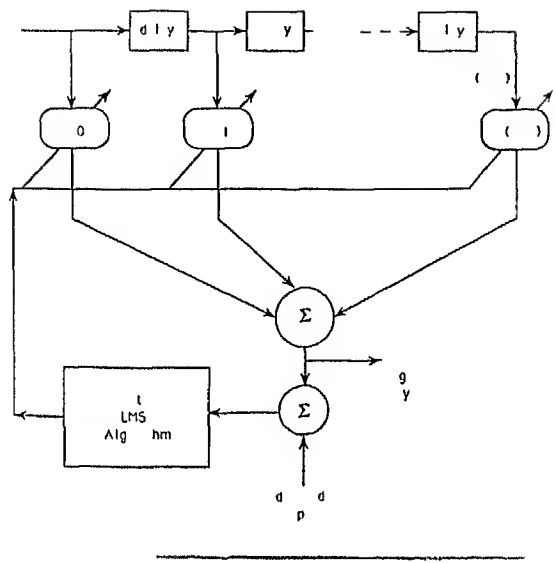


Figure 4.2 Block diagram of a tapped delay line adaptive filter [Ref 19]

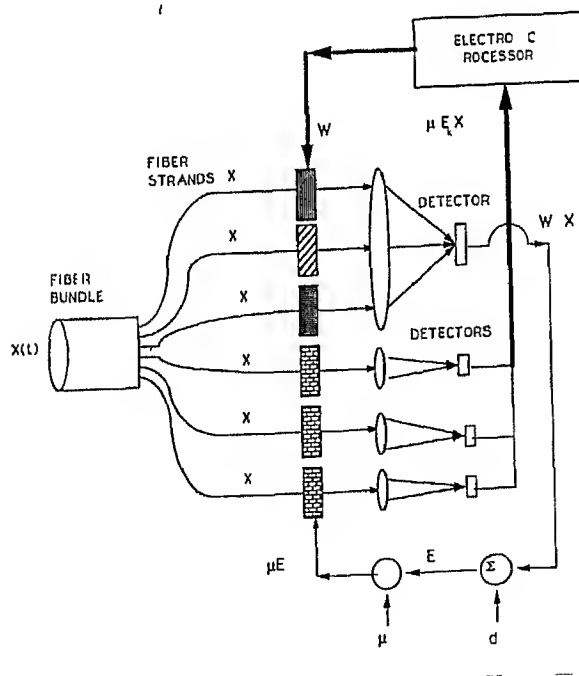


Figure 4.3 Block diagram of a fiber optic adaptive filter [Ref 19]

20 The main advantage of fiber optic adaptive filters is the possibility of directly using them in the processing of the lightwave signals in optical communication network

4 3 Spread spectrum fiber optic local area network using optical processing

Spread spectrum code division multiple access (CDMA) allows asynchronous multiple access to a local area network (LAN) with no waiting. The additional bandwidth required by spread spectrum can be accommodated by using a fiber optic channel and optical signal processing. A typical CDMA system using delay line signal processing is shown in fig 4 4 [21]. The transmitted data is encoded by the code generator. The coded data is

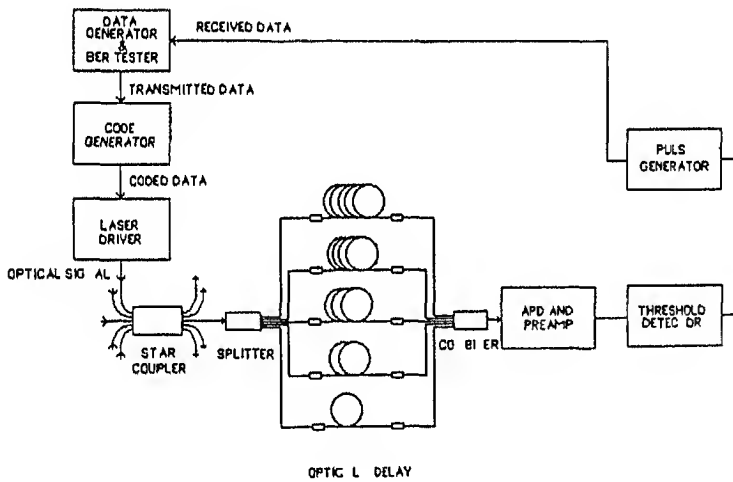


Figure 4 4 Block diagram of a CDMA processor [Ref 21]

injected into a fiber using a laser diode. At the receiver the incoming signal is split. The optical correlator then selectively delays the signals before recombining them. This processed signal impinges on an photodetector. The threshold detector checks the presence of the autocorrelation peak.

To take full advantage of the speed of optical processing it might be desirable to obtain all optical processor like one depicted in fig 4 5. A modelocked laser produces a low duty cycle, high intensity pulse stream at the data rate. This sequence of pulses is modulated by

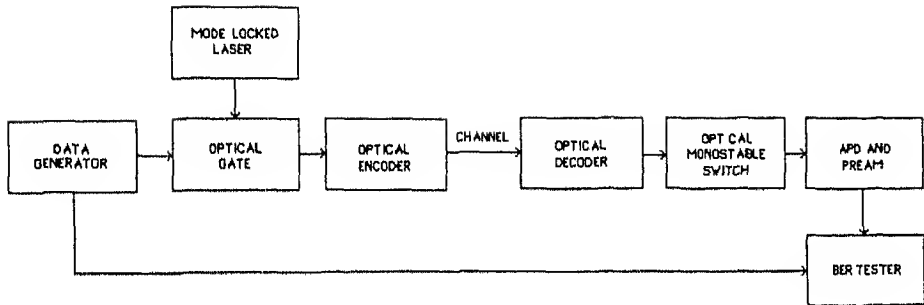


Figure 4.5 Block diagram of a system using both optical data encoding and decoding [Ref 21]

in optical gate, such as a directional coupler switch, which was driven by the information waveform. Using optical fiber delay lines, each short laser pulse generates the appropriate code sequence. At the receiver, correlation is performed by optical fiber delay lines in the way described earlier. In order to reduce the bandwidth requirements of the detector, the narrow autocorrelation peak is used to trigger a bistable or a monostable optical switch, which decay time equal to the bit width. The slowly decaying signal is detected and processed at the rate of the original data.

4.4 Spectral analysis of radio-frequency signals

Spectral measurement of narrow band optical signals can be done using a tapped delay line scheme. Temporal variations of an input signal are linearly converted into spatio temporal variations across a coherent array of optical radiators via a tapped delay line waveguiding structure. The diffraction pattern resulting from the field emitted by this array will exhibit frequency dependent regions of constructive interference. The waveguiding structure shown in fig 4.6 converts an input optical field into an array of outputs representing time delayed versions of the input, the delay time being proportional to the position X_1 , along the array, at $Z=0$. Such a device would permit the spectral analysis of very fast quasi monochromatic optical signals in real time without scanning [22].

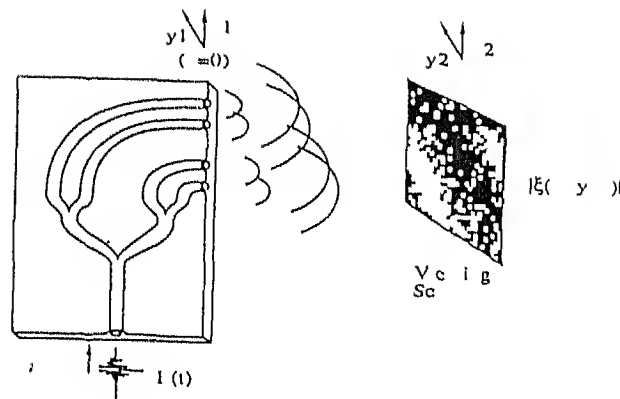


Figure 4.6 Block diagram of tapped delay line spectrum analyzer [Ref 22]

4.5 Transversal filter realization with non-uniform tap spacings

Using the fiber optic tapped delay line, one can realize a transversal filter with non uniform tap spacings. The non uniformity in the structure may decrease the number of taps and hence the cost for the same frequency response specifications. Further by exploiting the non uniformity in the transversal filter structure we can realize fiber optic transversal filter with only positive tap weights, which will remove the difficulty of optically realizing the negative tap weights.

Chapter 5

Conclusions

We have considered the design of a fiber optic tapped delay line transversal filter. The filter is fabricated following fiber bundle approach and the frequency response of the filter is measured. In such a realization, issues like non uniform coupling of light among fibers, bending loss, fiber loss and bandwidth limitations of transmitter and receiver circuits are important. We have considered all these issues in details and obtained the expected frequency response of the filter. When measured experimentally, the measured frequency response was found to be matching closely to the theoretical response.

Considering the perturbing effects as in section 3.2, we have seen that the effect of non uniform coupling and bandwidth limitations of transmitter and receiver circuits are much more severe than the effect of bending and fiber losses. One should choose a transmitter and receiver with sufficiently high bandwidth. Bending loss is also related with the issue of packaging of the filter.

To make a compact package, one needs to bend the fibers with a smaller radius of curvature and in that case bending loss becomes more. To deal with the specific case of our realization, when the diameter of bend was 15 cm, we needed to make 126 loops to accommodate all the fibers. The required height of the cylinder on which the fibers are wrapped is around 80 mm. So the required width and height of the box is atleast 15 cm and 80 mm respectively. The length of the box depends on the length of the shortest fiber. By reducing the loop diameter one can reduce the width of the box, but in that case bending loss will be more. We measured the bending loss for a loop of diameter 5 cm and it was approximately 6 dB more than the bending loss for a loop of diameter 15 cm. It is upto the user to make a suitable compromise between the box dimension and the bending

loss

The bending loss, fiber loss and the non uniform coupling of light into the fibers change the tap weights of the filter. But one can exploit these effects to restore the original tap weight values in the following way. Instead of keeping all the fibers at the same plane in the LED side in which all the fibers are separated by the same amount from the source we can place them with varying distances from the source. Fixing the longest fiber at the central position in the bundle acts in restoring the original values of the tap weights. The central fiber being the longest one, introduces the maximum amount of bending and fiber losses. On the other hand, because of its specific position in the bundle it receives more light power from the source. These two things act against each other and nullify the effect of the non uniform coupling to some extent.

Our work can be extended in the direction of achieving tap weights other than zero and one. For that, the fibers can not be tied up in the detector side like what we have done in our case. The fibers should be spatially distributed and a focussing lens is needed to focus the individual lights from the fiber at the detecting area. Even when all the weights are binary, but the number of fibers in the bundle is large, one may need to focus the individual lights from the fibers. Otherwise, to collect the light from all the fibers at the same detecting area, detector with larger area is needed and such a detector will restrict the bandwidth of the system.

Lastly, extension of this idea of fiber bundle based filter to the realization a filter with non uniform tap spacing is very straight forward. As we mentioned in Chapter 4 non uniform tap spacing requires lesser number of taps than that is required in case of uniform spacing of taps. It might also help to get all the tap weights as positive. Because of lesser number of taps, this particular cost effective approach of realizing a fiber optic transversal filter that we have followed might be suitable for the realization of filters with non uniform tap spacings.

Bibliography

- [1] D D Buss, R W Broderson, and C R Hewes "Charge coupled devices for analog signal processing" Proc IEEE Vol 64 p 801, 1976
- [2] G D Boyd, I A Goldien, and R N Thurston "Acoustic wave guide with a cladded core geometry" Appl Phys Lett , Vol 26 p 31, 1975
- [3] I I Clambornic G S Kino, and E Stein "Special Issue on Surface Acoustic Waves Proc IEEE, Vol 64, p 579, 1976
- [4] J D Adam, and M R Daniel "The status of magnetostatic devices " IEEE Trans Mag , Vol MAG 17, p 2951, 1981
- [5] J T Lynch, R S Withers, A C Anderson, P V Wright, and S A Reible "Multigigahertz bandwidth linear frequency modulated filters using a superconductive stripline ' Appl Phys Lett , Vol 43, p 319, 1983
- [6] K Wilner and A P Vanden Hauvel "Fiber optic delay lines for microwave signal processing " Proc IEEE, Vol 64, p 805, 1976
- [7] K P Jackson, S A Newton, B Moslehi, M Tur, C C Cutler, J W Goodman, and H J Shaw "Fiber optic delay line signal processing " IEEE Trans Microwave Theory Tech MTT 33, p 193, 1985
- [8] S A Newton, J E Bowers, and H J Shaw "Single mode fiber recirculating delay line " Proc SPIE, Vol 326, p 108, 1982
- [9] S A Newton, R S Howland, K P Jackson, and H J Shaw "High speed pulse train generation using single mode fiber recirculating delay lines " Electron Lett , Vol 19, p 756, 1983

- [10] J E Bowers, S A Newton, W V Sorin, and H J Shaw "Filter response of single mode fiber recirculating delay lines" Electron Lett, Vol 18, p 110, 1982
- [11] C Lee, R Atkins, and H Taylor "Reflectively tapped optical fiber transversal filters" Electron Lett, Vol 23, p 596, 1987
- [12] W Beck "Tapping optical fiber" Laser Focus, Vol 23, p 138, 1987
- [13] E Antonopoulos and R P Kenan "Integrated optical architectures for tapped delay lines" IEEE J Lightwave Technol Vol LT 8, p 1167, 1990
- [14] H F Kullmann "Transversal filters" Proc IRE p 302, 1940
- [15] Major H Singh, "M Tech Thesis, Design of a fiber optic analog link for video transmission" Dept of Electrical Engg IIT Kanpur, 1985
- [16] Gerid Keiser, "Optical fiber communication" McGraw Hill, New York, 2nd ed, 1991
- [17] D Gloger, "Bending loss in multimode fibers with graded and ungraded core index" Appl optics Vol 11, p 2506 1972
- [18] A H Cheein, "An introduction to optical fibers" McGraw Hill, Japan 3rd ed 1990
- [19] Anjan K Ghosh, P Paparao, and S Allen, "Design and performance optimization of fiber optic adaptive filters" Appl Optics, Vol 31, p 1826, 1991
- [20] Anjan K Ghosh, J Barker, and P Paparao, "Design of least mean square based adaptive optical equalizer" Optics Communications, V 91, p 280, 1992
- [21] P R Prucnal, T R Gan, and M A Santoro, "Spread spectrum fiber optic local area network using optical processing" IEEE J of LT V LT 4, No 5, p 547 1986
- [22] E Ranalli, and Henry P Lee, "Tapped delay line spectrum analyzer" Optics Comm, Vol 104, p 13, 1993

EE 1595 M RAY-FAY3



A121324